ABSTRACT

Title of Thesis: GEOTECHNICAL CHARACTERIZATION OF BALTIMORE DREDGED SEDIMENTS AS AN INFILTRATION BERM MATERIAL ON HIGHWAY SLOPES

Eren Kaya

Master of Science, 2024

Thesis Directed By: Professor Ahmet H. Aydilek
Department of Civil and Environmental Engineering
University of Maryland

Baltimore Harbor dredged material has limited use in common geotechnical construction due to its soil composition. It has low shear strength for foundation applications and lack of plasticity makes it an undesirable material for seepage barrier applications. Vegetated infiltration berms, used for regulating stormwater discharge, can be suitable for beneficial reuse of the dredged materials. The scope of this research is to appropriateness of the dredged material for construction an infiltration berm that has sufficient slope stability and provides total infiltration in less than 72 hours. Unconfined compression tests, constant head permeameter tests and unsaturated hydraulic conductivity tests were conducted on the dredged material and its blends with straw, sand, and recycled glass aggregate. All amendments were chosen due to their potential of reducing infiltration time, increasing hydraulic conductivity and as well as increasing the available water content (AWC) to promote vegetation. The effects of different amendments on soil water characteristics curves were examined and related to the vegetation through percent green cover data. Results obtained through testing were implemented in finite element analysis programs, SLOPE/W and SEEP/W, to analyze slope stability and seepage behavior of the berm, respectively. Common berm geometries along with different subgrade conditions were considered during modeling. Straw amended dredged material provided adequate hydraulic conductivity, met the required minimum infiltration times, and acceptable AWC to promote vegetation, without experiencing any slope stability or piping failures.

GEOTECHNICAL CHARACTERIZATION OF BALTIMORE DREDGED SEDIMENTS AS AN INFILTRATION BERM MATERIAL ON HIGHWAY SLOPES

by

Eren Kaya

Thesis submitted to the Faculty of the Graduate School of the
University of Maryland, College Park, in partial fulfillment
of the requirements for the degree of
Master of Science
2024

Advisory Committee:
Dr. Ahmet H. Aydilek, Chair
Dr. Sherif M. Aggour, Committee Member
Dr. Allen P. Davis, Committee Member

Dedication

I dedicate this thesis to my family, who have been the safest of ports through all the storms I had to endure.

Acknowledgements

I hereby thank my advisor, Dr. Ahmet H. Aydilek, for his continuous guidance and understanding. Thank you to the committee members, Dr. Sherif M. Aggour and Dr. Allen P. Davis for their time and efforts. Thank you to Dr. Aslı Yalcin Dayioglu for believing in me and Dr. Mustafa Hatipoglu for providing a helping hand whenever and wherever needed. Finally, a special thank you to my dearest friend Kaan and dear teacher Mr. Gunes for believing in me unconditionally.

Table of Contents

List of Figures

List of Tables

Chapter 1

Introduction

Dredged material management has become an issue of importance as the stockpiled amount increases each year. Approximately 3.3 million cubic meters of sediment is dredged annually from the Port of Baltimore and nearly 55 million cubic meters needs to be stored in designated facilities in the next 20 years (MDE, 2019). Previously, the material was stored and enclosed within Hart-Miller Island until it was filled to its maximum capacity in 2009 (Francingues et al.,2011). Due to Maryland state regulations developed in 2005, it was not permissible to deposit the material outside the harbor area, and since then the material has been stored at the Cox Creek Dredged Material Containment Facility, positioned to the south of the Scott Key Bridge on the western bank of the Patapsco River (Malasavage et al.,2012). The Cox Creek site, initially having a capacity of 4.9 million cubic meters that had almost filled completely, saw an expansion project starting in 2017 which increased the storing capacity to 8.6 million cubic meters (MPA, 2020). This constant one-way traffic of the dredged material to the facility makes the need for a reuse method apparent and urgent.

MPA is interested in viable alternatives to process and discover innovative reuse methods for the dredged sediments. The significance of this dredging operation partially stems from the desire to attract cargo from the Panama Canal expansion (Houlihan et al., 2020). It is imperative to develop high-production, cost-efficient processes to diminish existing inventories and facilitate the ongoing transfer of material from harbor dredging operations without exceeding the containment's defined capacity.

Given the significance of the Port of Baltimore to Maryland's and nation’s economic future, the planned expansion of the Port underscores the importance of exploring a variety of innovative options for reusing the dredged material.

One of the reuse options for DM is to utilize it in construction of vegetated earth berms (VEBs), also known as infiltration berms, to help with the regulation of surface water runoff in highway slopes. With the ongoing effects of climate change in Maryland, the state faces heightened risks of flooding across various areas including agricultural lands, urban regions, and highways (Joyce and Scott, 2005). Flood events may arise from excessive rainfall, and infiltration berms offer a practical option for mitigating these risks. They can be strategically placed on slopes, such as highways, as part of erosion control strategies, redirecting stormwater runoff and mitigating the impact of flooding. These berms can help increase infiltration, reducing the likelihood of excessive stormwater runoff on highways and highway slopes (MDE, 2000). Typically, infiltration berms are constructed using compacted soils devoid of roots, large rocks, or vegetation, and can be designed to be impermeable or slightly permeable, allowing for gradual water release and filtration of collected water (MDE, 2000).

Geotechnical design of a VEB requires understanding of shear strength and hydraulic conductivity of the construction materials used. Hydraulic properties of the dredged material, under both fully and partially saturated conditions, need to be determined to estimate generated pore pressures and exit gradients as well as the time it takes the ponding water to infiltrate the berm structure. Infiltration time, which is

also linked to geometry of the berm, is an important parameter as the berms are required to be vegetated and plants need water for growth.

The objectives of the study are to define geotechnical properties of the Baltimore Harbor dredged material and its blends as knowledge on these parameters are needed for seepage and stability analysis. To respond to this need, a series of laboratory tests were performed on the dredged material and its blends to analyze their undrained shear properties. Hydraulic conductivity tests were conducted under fully- and partially saturated conditions, and the obtained geotechnical parameters were used to conduct seepage and slope stability analyses under varying geometries and upstream water levels. Recommendations were developed to accommodate different design scenarios under varying geometries and site conditions.

Chapter 2

Materials and Methods

2.1 Materials

Baltimore Harbor dredged material was the material of focus. The dredge material was procured from Cox Creek Dredge Material Containment Facility in Curtis Bay, Maryland. The average water content of the collected dredged material was 18%. The materials were then sealed in airtight plastic buckets and stored in Whiting-Turner Infrastructure Engineering Laboratories at the University of Maryland, College Park.

Initial environmental analysis conducted by Smith (2024) showed that addition of amendments is necessary to stabilize the dredge materials; recycled glass aggregate (G), sand (S) and wheat straw (W) were selected as amendments. Upon conducting a series of pocket penetrometer tests (WK27337) and water content measurements (ASTM D2216-19), the following percentages were used to amend the dredged material: 5% sand, 10% sand, 5% recycled glass aggregate, 10% recycled glass aggregate, 0.5% wheat straw and 1% wheat straw.

All materials were dried at 100^{o}C for 24 hours before processing and mixing with amendments. The processing consisted of breaking big clumps of dried dredged material with a mallet into smaller particles. Wet sieve analysis (ASTM C92-95) and SALD-2300 particle size analyzer (Shimadzu Corp., Somerset, NJ) were used to determine the sand, silt and clay percentages (which are consistent with the ones in the United States Department of Agriculture Soil Classification System). Grain size distributions of the materials determined using the AASHTO T-88 procedure are given in Figure 1.

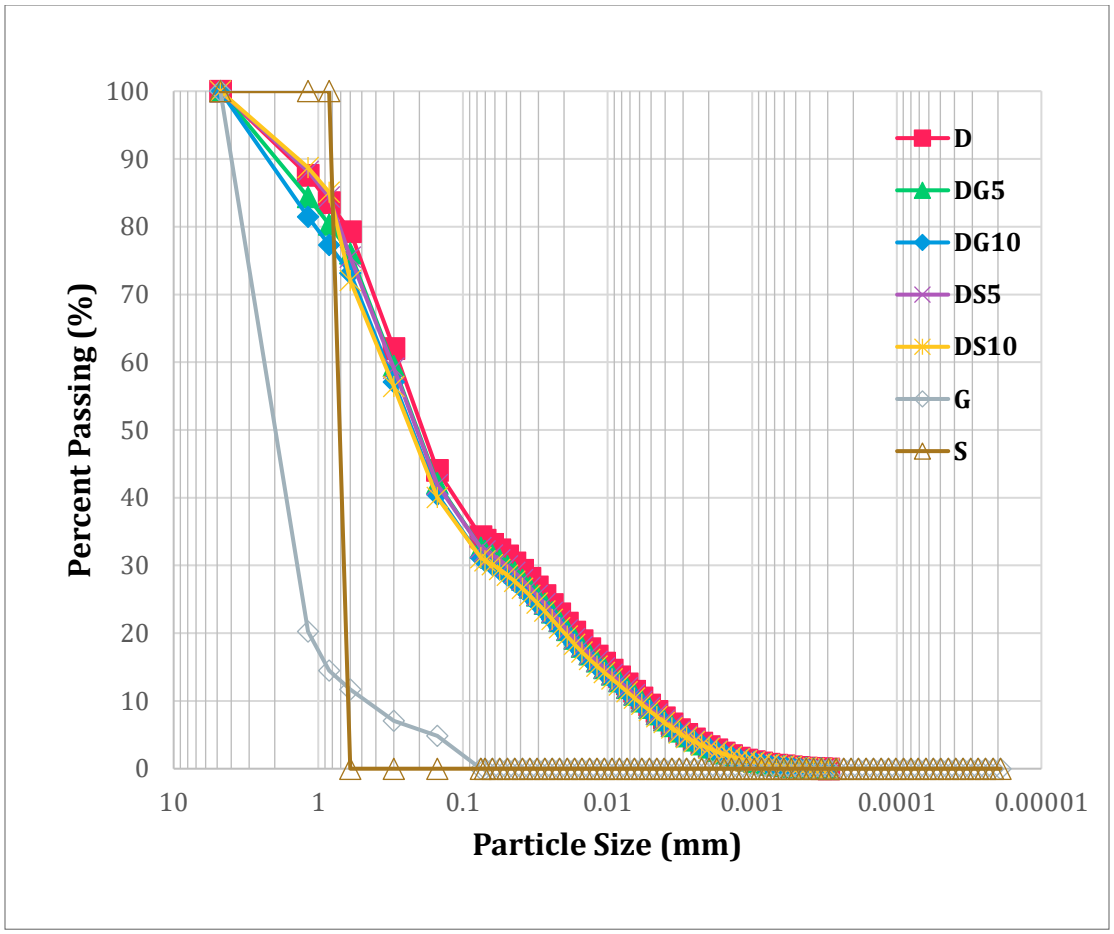

Figure 1. Grain size distributions of the materials tested

S and G had the highest percentages (100%) of sand-size particles (i.e., 75 µm-4.75 mm) with no fines contents. D had the highest percentage of fines (<0.075 mm) content (34.2%) and the lowest sand-size content (65.8%). Table 1 lists the index properties of the materials tested. The plasticity index (PI) value (ASTM D4318) was 12 for D, DS5 and DS10. Recycled glass aggregate amended sediments could not tested for plasticity due to broken glass pieces. All materials were classified per Unified Soil Classification System (USCS) and United States Department of Agriculture (USDA) Classification System and these are summarized in Table 1.

Table 1. Index and compaction properties of the materials tested

Material	Composition	Sand (%)	Silt (%)	Clay (%)	C_c	C_u	LL	PI	G_s	USDA Classification	USCS Classification
D	100% dredged material	65.8	30.4	3.8	1.11	48.61	35±3	12±2	2.65±0.02	Sandy Loam	Clayey sand (SC)
S	100% testing sand	100	0	0	0.98	1.12	NA	NA	2.65	Sand	Poorly Graded Sand (SP)
G	100% recycled glass aggregate	100	0	0	1.66	4.73	NA	NA	2.21±0.06	Sand	Poorly Graded Sand (SP)
DS5	%5 percent sand amended	67.4	29	3.6	1.37	53.71	35±3	12±2	2.65±0.02	Sandy Loam	Clayey sand (SC)
DS10	%10 percent sand amended	68.9	27.6	3.5	1.73	56.87	35±3	12±2	2.65±0.02	Sandy Loam	Clayey sand (SC)
DG5	%5 percent glass amended	67.4	29	3.6	1.38	53.22	NT	NT	2.63±0.03	Sandy Loam	Clayey sand (SC)
DG10	%10 percent glass amended	68.9	27.6	3.5	1.79	55.19	NT	NT	2.61±0.04	Sandy Loam	Clayey sand (SC)

Notes: C_c: coefficient of curvature, C_u: coefficient of uniformity, PI: plasticity index, LL: liquid limit , NA: not applicable, G_s: specific gravity, , NT: Not tested due to nature of the material.

2.2 Methods

2.2.1 Shear Tests

Unconfined compression tests (ASTM D2166-06) were performed on dredged material and its blends by using the GEOTAC Unconfined Compression System. The specimens were compacted in a split compaction mold at their natural water content (w=18%) and a bulk density of 1.4 g/cm^3. This bulk density was selected per USDA guidelines as higher bulk density values are reported to cause restrictions to root growth, and poor movement of air and water through the soil (NRCS 2019) The cylindrical specimens had a height of 146 mm, and a diameter of 71.1 mm, and were strained at a constant strain rate of 1% per minute during the shear tests.

2.2.2 Hydraulic Tests

2.2.2.1 Saturated Hydraulic Conductivity Tests

In order to determine saturated hydraulic conductivities of the materials, constant-head tests were performed in bubble-tube permeameters and by following the procedures listed in ASTM D2434. Cylindrical samples with heights and diameters of 76.2 mm were compacted to a target dry density of 1.4 g/cm^3 in acrylic testing molds and the tests were continued until the termination criteria outlined ASTM D5084 is achieved. A minimum testing duration of 60 minutes was selected. The bubble tube permeability test setup allows the application of very low hydraulic gradients as well as accommodates high flow rates that can be encountered while testing permeable specimens, and significantly minimizes sidewall leakage. Due to its unique design, the use of valves, fittings and smaller diameter tubing is eliminated and head losses that interfere with the test measurements are avoided (Topaloglu et al. 2024). Upon

compacting the sample in the mold, the permeameter was placed in a water bath to keep the tail elevation constant. Before starting the test, the brim of the bubble tube was closed, and the reservoir was filled with water using a vacuum pump. When the level became stable, the test was started by opening the brim of the bubble tube. The total head difference through the specimen (ΔH), which was kept constant during the test, was equal to height difference between the bottom of the bubble tube and the top of the tub. The total flow rate through the specimen was determined by noting the water elevation drop in the reservoir tube and multiplying it with the inner area of the reservoir tube minus the outer area of the bubble tube. Triplicate tests were performed on each mixture. Finally, the vertical hydraulic conductivities were calculated using Darcy's law.

2.2.2.2 Unsaturated Hydraulic Conductivity Tests

For the unsaturated hydraulic conductivity testing, HYPROP testing setup (Meter Group, Inc, Pullman, WA) was used (Figure 2). Specimens of the dredged material were compacted at their natural water contents to a bulk density of 1.4 g/cm^3 and saturated afterwards by leaving the compacted specimens in a pool of water 1 cm lower than the surface level of the specimen. HYPROP system gathers data points within the suction range of 0 to 100 kPa, generating a detailed soil-water characteristic curve (SWCC). Unlike other methods utilizing a vacuum to introduce matric suction to the system, HYPROP employs a simplified evaporation method. Tensiometers (Meter Group Inc, Pullman, WA) located at depths of 1.25 cm and 3.75 cm from the sample surface were used to measure pressure heads. Each sample is placed on precise balances to be weighed to determine the evaporation rate, by

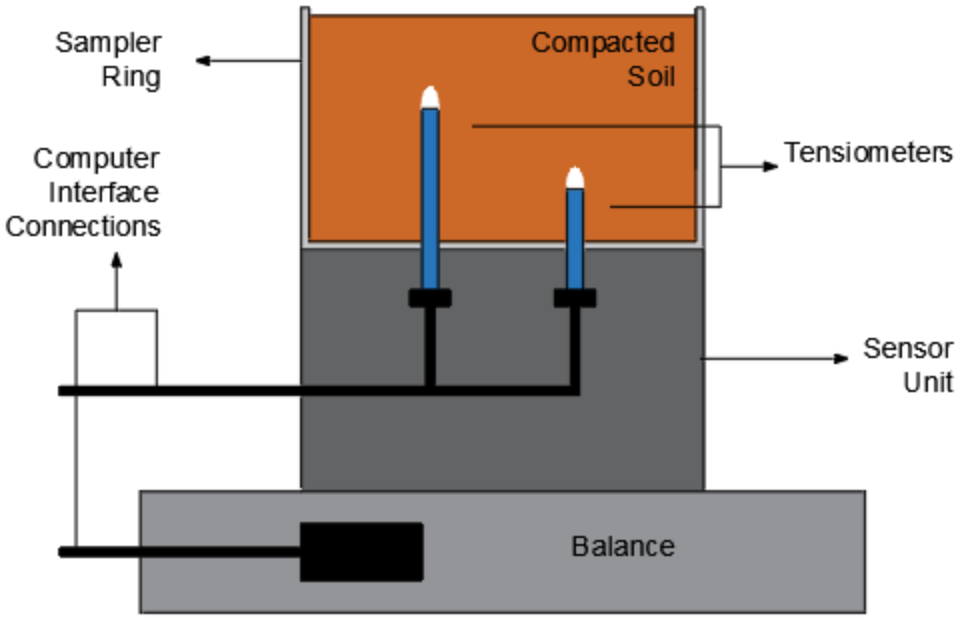

(a)

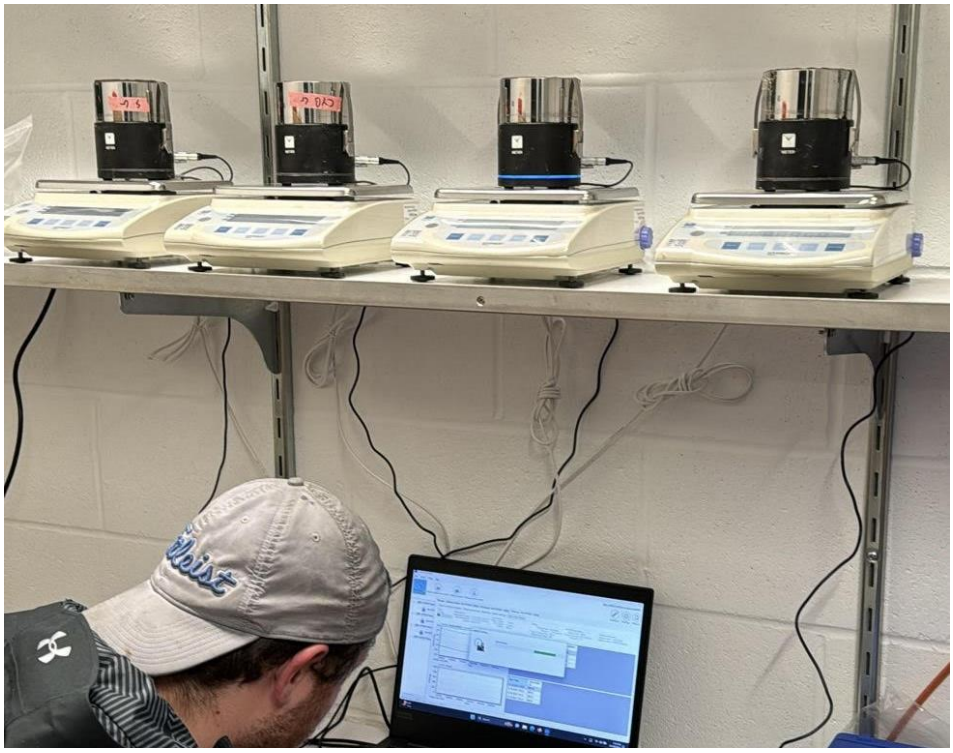

(b)

Figure 2. (a) Schematic of a HYPROP cell and (b) picture of HYPROP setup in the geotechnical engineering laboratory

relating the change in weight to the change in volumetric water content. Data is collected and simultaneously logged to the file with a data point being collected every minute for the first hour and then every 10 minutes until the test concludes. Data analysis software LABROS SoilView Analysis is coupled with the HYPROP setup, and enables the user to try different curve fitting functions to the collected data points. The retention curve fitting function applied was the unimodal constrained model proposed by van Genuchten (1980), which is expressed as follows:

$$S_e(h) = \frac{\theta(h)-\theta_r}{\theta_s-\theta_r} = \left[\frac{1}{1+(\alpha|h|)^n}\right]^{1-\frac{1}{n}} \qquad (1)$$

where, S_e is the effective saturation [-], θ_s is the saturated water content [cm^3cm^{-3}], θ_r is the residual water content [cm^3cm^{-3}], α is a shape parameter [cm^{-1}] which is linked with the inverse of the air-entry pressure, n is a shape parameter [-] that is related to bending of the retention curve, and h [cm] is the pressure head.

The relationship between unsaturated hydraulic conductivity and volumetric water content was determined, and the van Genuchten/Mualem model (Mualem 1976, van Genuchten 1980) was employed as the fitting function for conductivity:

$$K(h) = K_{sat}(1+(\alpha|h|)^n)^{\tau(1/n-1)}[1-(\alpha|h|)^{(n-1)}[1+(\alpha|h|)^n]^{1/n-1}]^2 \qquad (2)$$

where, K_{sat} is the saturated hydraulic conductivity, and τ [-] is tortuosity.

The laboratory-obtained soil water characteristic curve (SWCC) defines wilting point (WP), field capacity (FC) and available water content (AWC) of each material. Field capacity (FC) is the soil moisture level at which excess water has drained away, while the wilting point (WP) is the minimum soil moisture required to prevent plant wilting (Kirkham, 2005; Minasny and McBratney, 2018). The available water capacity

(AWC) for each material was calculated as the difference in water content between the field capacity (FC) and the wilting point (WP). All materials in this study were classified as having a coarse texture according to the USDA soil classification system. In line with the recommendations of Colman (1947), Jamison and Kroth (1958), Ratliff et al. (1983), and Huntington (2007), FC and WP were defined as the water contents at soil water potentials of -10 kPa and -1500 kPa, respectively. Figure 3 illustrates the parameters for FC, WP, and AWC.

2.2.3 Slope Stability and Seepage Analysis

Numerical analysis of slope stability and seepage were conducted using GeoStudio SLOPE/W and SEEP/W. The berm was numerically modeled using the input data obtained in the laboratory tests. The design guidance in Maryland Stormwater Design Manual regarding infiltration berms as issued by Maryland Department of the Environment (MDE) states that berms shall be level and be asymmetric in shape. The crest width of the berm should be 0.62m, and the berm slopes should be shallow, 2:1 ratio being the steepest; these berms shall not be constructed on slopes greater than 10% to avoid erosion (MDE, 2000).

The berms were assumed to sit on one of two common foundation soils in Maryland, named Subgrade 1 and Subgrade 2 herein. The geotechnical properties of these soils, as reported by Dayioglu and Aydilek (2019), are provided in Table 2.

Side slopes of 2H:1V, 3H:2V and 3H:1V, subgrade slopes of 0%, 5% and 10% were selected. Furthermore, a secondary layer of subbase was introduced between the infiltration berm and the subgrade (at thicknesses of 0.31 and 0.62 m),

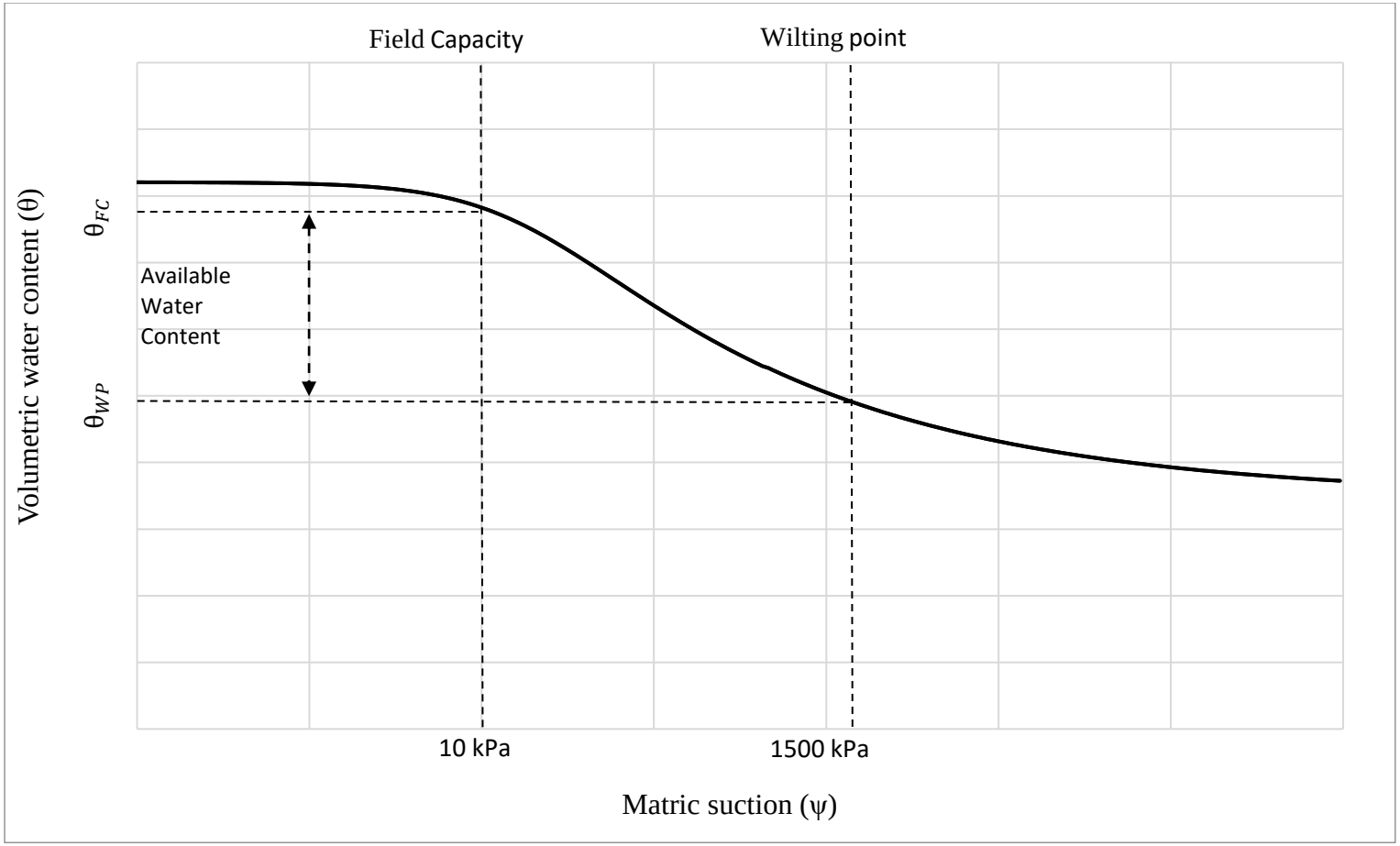

Figure 3. Exemplary soil-water characteristics curve with FC, WP and AWC

Table 2.Geotechnical properties of the common foundation soils in Maryland.

Material	G_s	FC	LL	PI	USCS Classification	Hydraulic conductivity, K_{sat} (cm/s)
Subgrade Soil 1	2.68	53	24	6	CL-ML	$7.1x10^{-6}$
Subgrade Soil 2	2.68	66	30	12	CL	$1.1x10^{-6}$

Notes: G_s: specific gravity, FC: fines content, LL: liquid limit, PI: plasticity index, K_{sat}:saturated hydraulic conductivity.

with the idea of increasing dredged sediment usage throughout the berm design (Table 3, Figure 4). Based on literature review, the main design criteria for the infiltration berm in the scope of this research were:

- Sufficient slope stability against rotational failures
- Low exit gradients to avoid piping effect.
- Infiltration times shorter than 3 days (72 hours) to make sure flies do not lay their larvae, i.e., do not create a swamp system.

Seepage Analysis

SEEP/W (Seequent 2024) was used to determine exit gradients and seepage velocities within the berm structure, subbase, and subgrade. Steady-state models in SEEP/W were created in accordance with the manufacturer's manual (Geo-Slope International 2012). The critical gradient (i.e., the gradient where soil particles start being suspended in water and therefore mobilized) was calculated for each material using

$$i_c = \frac{\gamma_{sat} - \gamma_w}{\gamma_w} \quad (3)$$

where i_c is the critical hydraulic gradient, γ_{sat} is the saturated unit weight, and γ_w is the unit weight of water (Briaud et al. 2016). The maximum exit gradient, i_{exit} obtained for a particular material using the SEEP/W analyses (Figure 5) was compared to its critical gradient to calculate FS_{piping}

$$FS_{piping} = \frac{i_c}{i_{exit}} \quad (4)$$

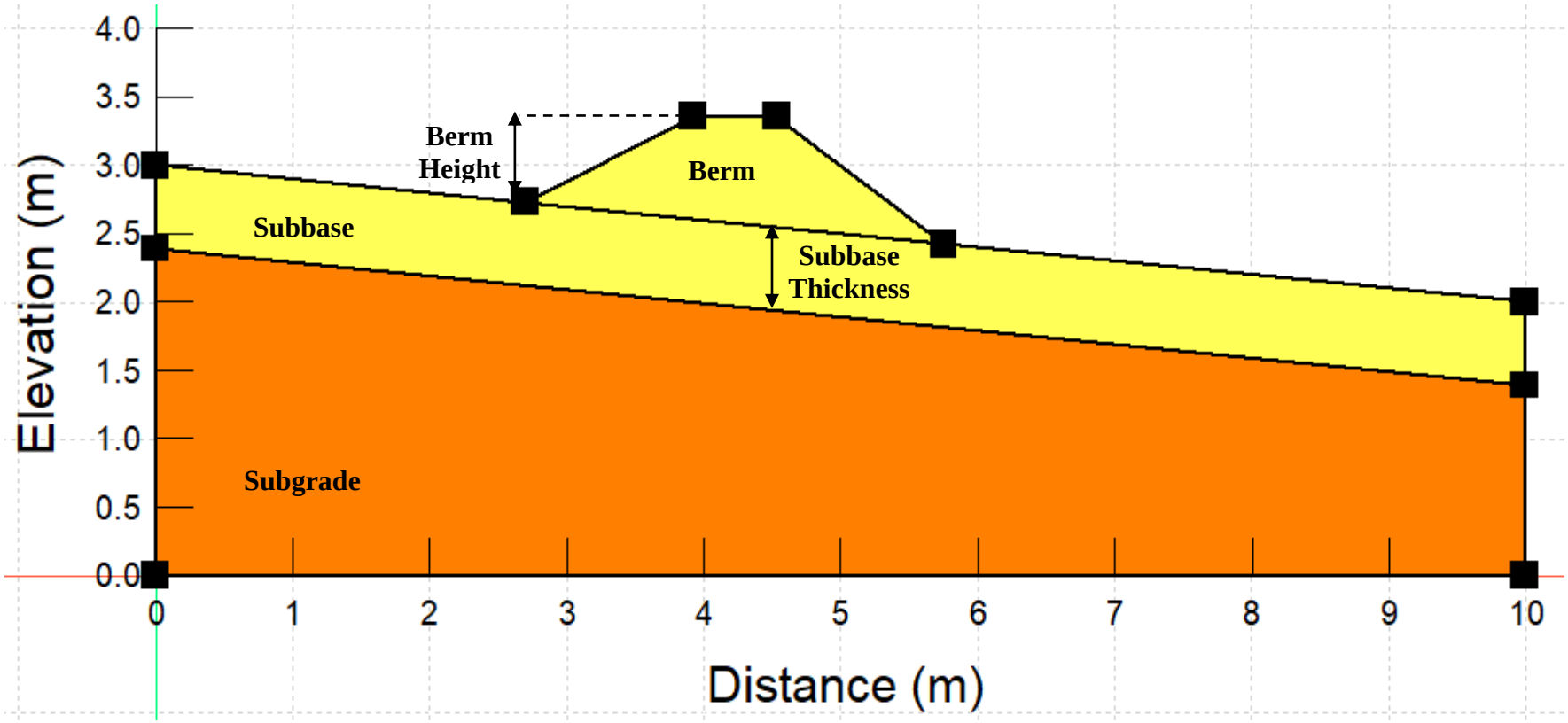

Figure 4:*0.62*-m high infiltration berm model with side slopes of 2H:1V and a subgrade slope of 10H:1V

Table 3. Dimensions and material types examined for berm design.

Berm Test	Berm Material	Side Slope	Subgrade Slope	Subgrade Type	Subbase Thickness (m)	Data Collected	FS	Design FS	Software	Numerical Model
Downstream Slope Stability	**D, DS5, DS10, DG5, DG10, DW0.5, DW1**	1H:1V, 3H:2V, 2H:1V	No slope, 20H:1V, 10H:1V	Subgrade 1, Subgrade 2	0, 0.31, 0.62	$FS_{downstream}$	$FS_{downstream}$	1.4	SEEP/W SLOPE/W	Steady State
Seepage Through Berm	**D, DS5, DS10, DG5, DG10, DW0.5, DW1**	1H:1V, 3H:2V, 2H:1V	No slope, 20H:1V, 10H:1V	Subgrade 1, Subgrade 2	0, 0.31, 0.62	i_{exit}	$FS_{piping} = \frac{i_c}{i_{exit}}$	1.5	SLOPE/W	Transient
Infiltration Time	**D, DS5, DS10, DG5, DG10, DW0.5, DW1**	1H:1V, 3H:2V, 2H:1V	No slope, 20H:1V, 10H:1V	Subgrade 1, Subgrade 2	0, 0.31, 0.62	$t_{infiltration}$	NA	NA	SLOPE/W	Transient

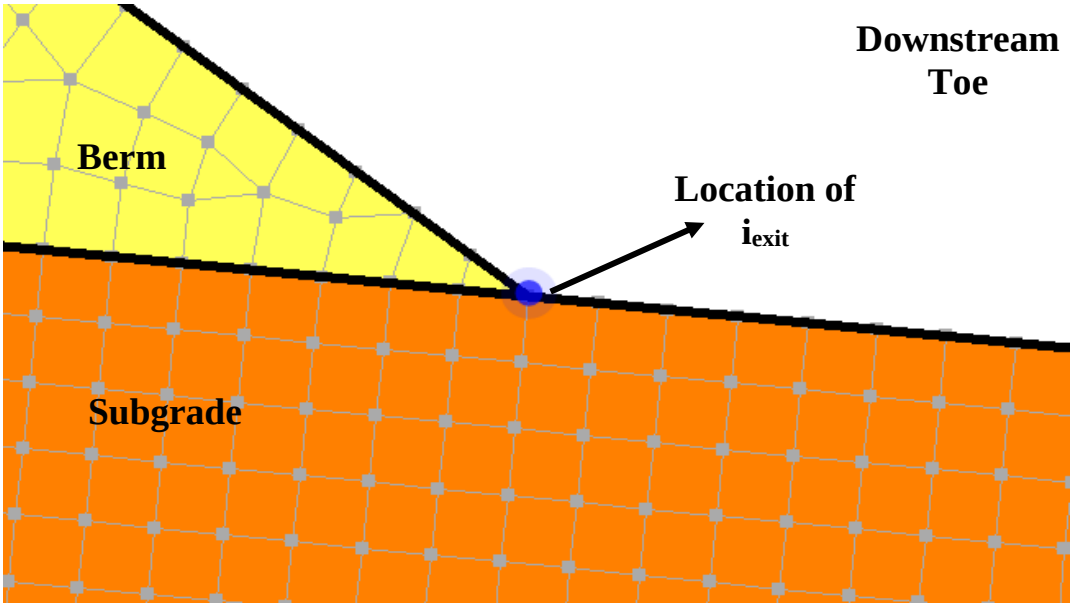

Figure 5. Location of exit gradient for seepage analyses.

The time it takes for the impounded water to infiltrate the berm should not exceed 72 hours, as it would carry the risk of acting as a swamp media for the flies to lay their larvae in (MDE 2000). An initial steady-state seepage analysis was first established. A transient seepage analysis was then assigned to the parent steady state seepage analysis to examine the time-dependent behaviour of the water impounded behind the berm by utilizing the unsaturated hydraulic conductivity parameters of the materials obtained through the HYPROP measurements. As the height of the berm is designated to be 0.62 m, the impounded water height was assumed to be brim-full as this would be the most critical condition during the berm design.

Slope Stability Analysis

SLOPE/W (Seequent 2024) was used to determine the factors of safety against rotational failures (Figure 6) for the proposed berm geometries and materials. The

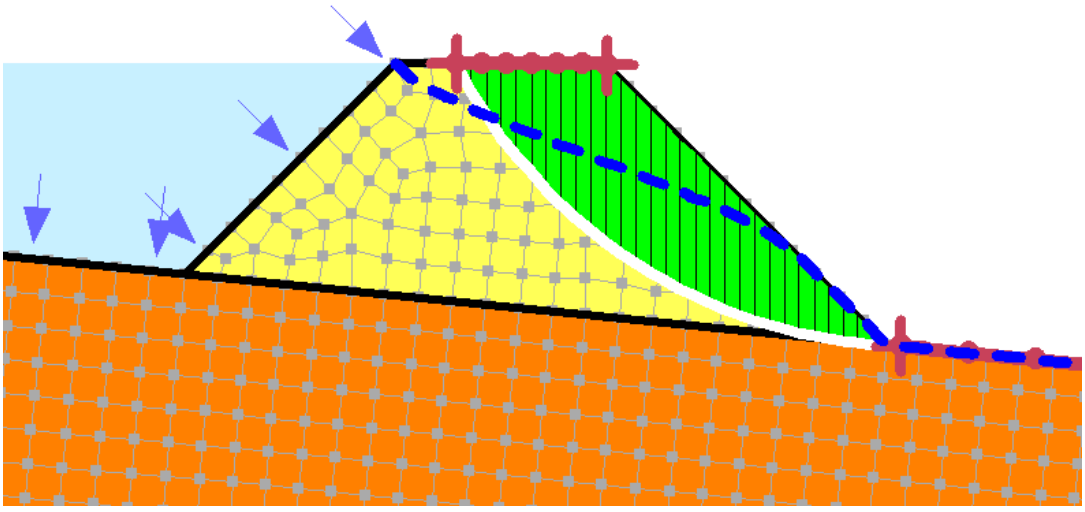

Figure 6. An example SLOPE/W showing most critical slip surface (in white) for a rotational failure analysis.

finite-element software uses the limit equilibrium method of slices and Morgenstern-Price method to calculate the factor of safety against failures for the user generated slip surfaces. For each geometry and soil type combination, the lowest factor of safety of that respective combination was selected as $FS_{downstream}$. Currently no design FS exists for slope stability of infiltration berms, and a design factor of safety of 1.4 was selected for downstream slope stability following the guidelines in Technical Release 210-60 Earth Dams and Reservoirs (NRCS, 2019) (Table A1, Appendix).

Chapter 3

Results and Analysis

3.1 Results of Shear Tests

The unconfined compression test results are given in Table 4. As expected, amending with sand or glass aggregate reduces unconfined compressive strengths by 1.5-1.7 times, whereas an increase in strength can be observed with straw addition (from 19.7 kPa to 26.5-36.7 kPa). Yetimoglu and Salbas (2003) found that amending sands with fibers increased the shear strength of the soil while reducing the stiffness. Fang et al. (2016) showed that both cohesion and friction angle of the soil increased with the addition of straw, with an amendment of 1% straw providing around 1.8 times increase in cohesion, consistent with the results obtained in the current study (Table 4). Similarly, Li et al. (2010) examined that saline soil with wheat and lime showcased higher unconfined compressive strength than saline soil treated with just lime.

Recycled glass aggregate has no effect on strain-at-failure while both sand and straw yield higher strains at failure, proportional to the amount of amendment material (Figure 7). The data presented in Figure 8 show that unconfined compressive strength is influenced by amendment amount; straw showing a positive correlation while sand and glass showing a negative one. The decrease in unconfined compressive strength with the increase in granular soil amendments can be explained as a reduction in cohesion. The addition of S and G separate clay particles from one another, causing less attraction between them (Alkroos et al.,2021). Another possible

Table 4. Summary of the unconfined compression tests

Material	Measured property		
	q_u (kPa)	c_u (kPa)	ε_f (%)
D	29.5 ± 4.3	14.8 ± 2.1	0.98 ± 0.10
DS5	26.2 ± 4.8	13.1 ± 2.4	1.46 ± 0.14
DS10	23.8 ± 3.9	11.9 ± 2.0	1.75 ± 0.21
DG5	27.2 ± 2.3	13.6 ± 1.2	1.02 ± 0.05
DG10	23 ± 2.9	11.5 ± 1.5	1.01 ± 0.17
DW0.5	53 ± 0.9	26.5 ± 0.5	1.61 ± 0.05
DW1	73.4 ± 1.2	36.7 ± 0.6	2.00 ± 0.03

Notes: q_u: unconfined compressive strength, c_u: undrained cohesion, ε_f: strain at failure.

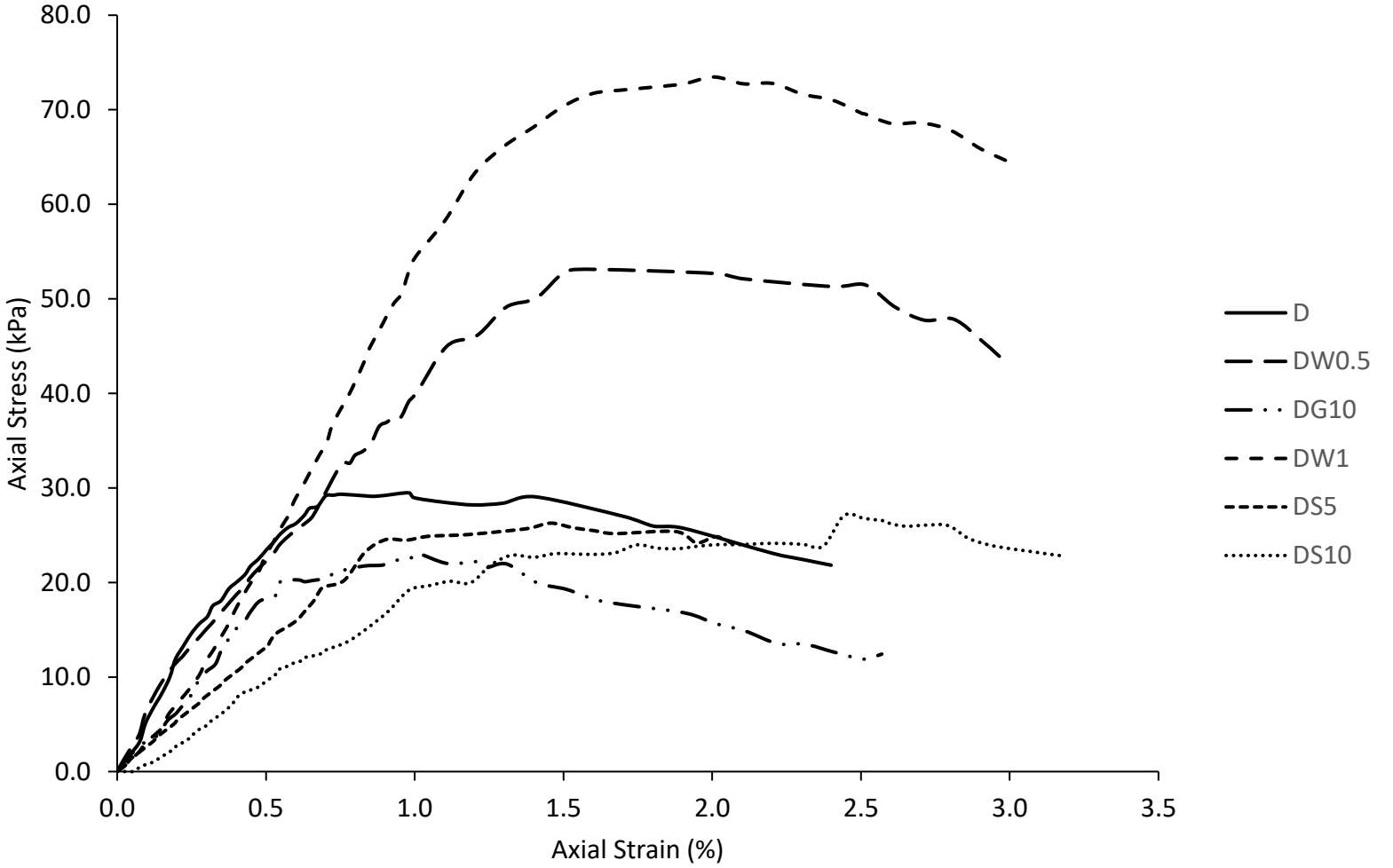

Figure 7. Stress versus strain behavior of dredged sediments amended with W, S and G.

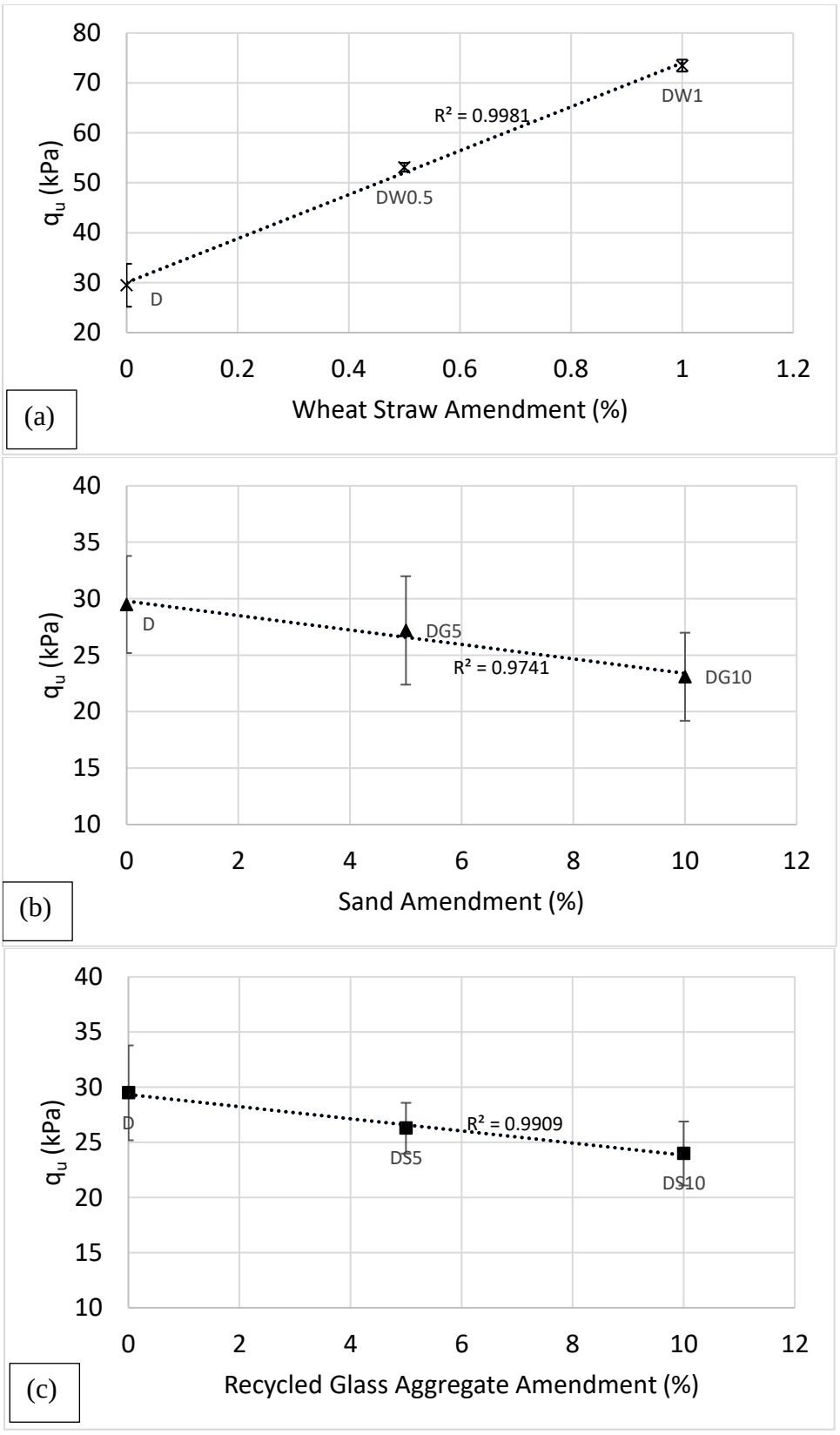

Figure 8. Effects of (a) W, (b) S and (c) G addition on unconfined compressive strength (q_u)

cause of the reduction in shear strength is due to an increase in material heterogeneity as well as the loss of sand particles while the specimen is being compressed (Khan et al. 2014). Amiri et al. (2018) also observed a decrease in cohesion, and an increase in friction angle, when kaolinite was amended with recycled glass aggregate to increase its workability.

3.2 Results of Hydraulic Tests

3.2.1 Saturated Hydraulic Conductivity Tests

Results of saturated hydraulic conductivity tests are summarized in Table 5. D has the lowest saturated hydraulic conductivity (K_{sat}=3.7 x 10^{-5} cm/s) while the highest saturated hydraulic conductivity value measured is for DW0.5 (K_{sat}= 3.6 x 10^{-4} cm/s). Increases in hydraulic conductivity were examined due to the addition of S, G and W.

Amending with 0.5% straw increased the saturated hydraulic conductivity by approximately 10 times whereas adding more straw (1%) decreased the hydraulic conductivity (Figure 9). These changes in hydraulic conductivity are attributed to changes in porosity and development of tortuous flow pathways inside the specimen (Figure 10). All materials were compacted to an initial bulk density of 1.4 g/cm^3 for hydraulic testing. Although the bulk density was the same across all samples, straw amended specimens had lower porosities due to their lower bulk densities and, thus, lower specific gravities. As the density of the wheat straw (0.097-0.18 g/cm^3; Zhang et al., 2012), is significantly lower than bulk density of the soil specimens prepared, 1.4 g/cm^3, the amount of space occupied by the straw decreases the overall porosity (n), resulting in n_{DW1} =0.40<$n_{DW0.5}$ =0.44< n_D =0.47. It is believed that at lower amendment percentages, i.e. DW0.5, the straw increased the void ratio and introduced

Table 5. Summary of the constant head permeameter test results

Material	Hydraulic Conductivity (cm/s)
D	$3.6 \pm 0.5 \times 10^{-5}$
DS5	$1.3 \pm 0.8 \times 10^{-4}$
DS10	$2.5 \pm 1.0 \times 10^{-4}$
DG5	$8.7 \pm 0.9 \times 10^{-5}$
DG10	$1.7 \pm 1.2 \times 10^{-4}$
DW0.5	$3.4 \pm 0.4 \times 10^{-4}$
DW1	$6.4 \pm 1.3 \times 10^{-5}$

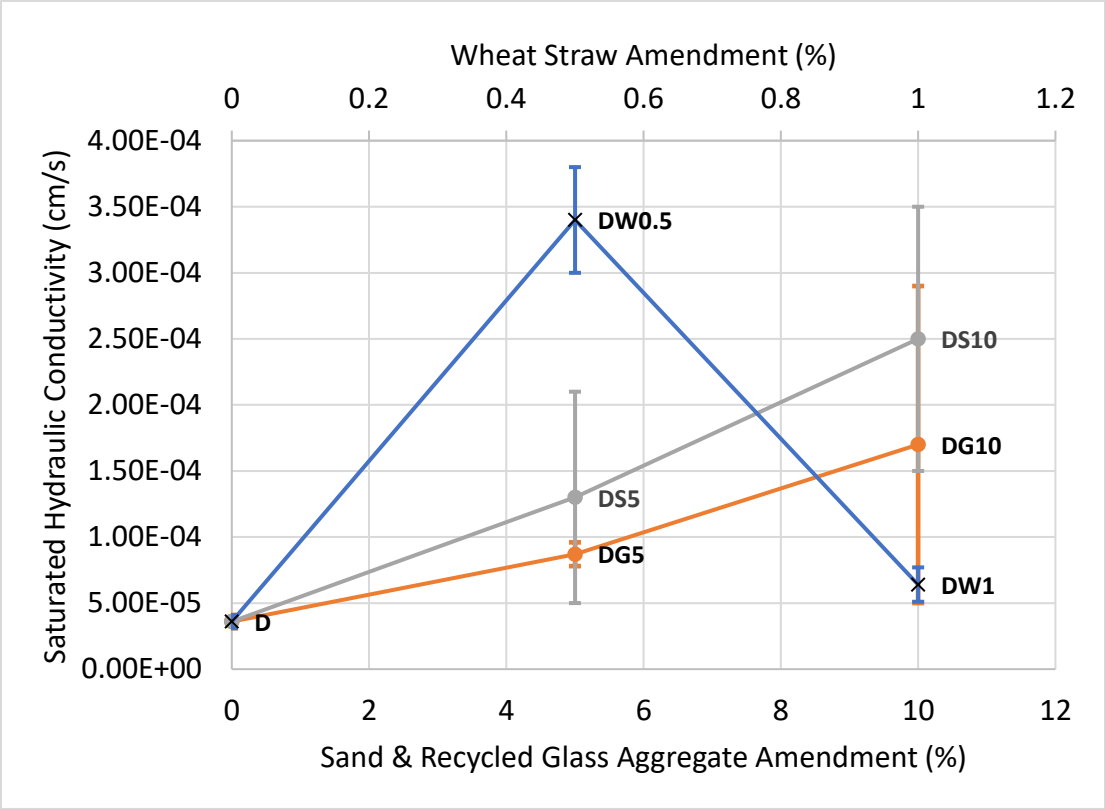

Figure 9. Change in K_{sat} with respect to amendment type and amount.

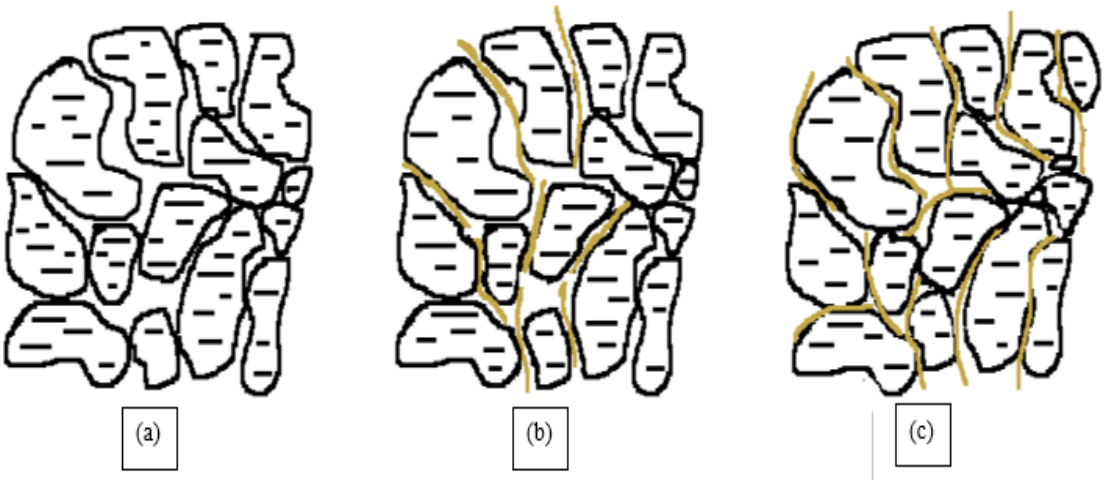

Figure 10. Schematic diagram of (a) D, (b) increased flow channels due to small amount of straw addition in DW0.5, and (c) the least amount of porous space and a mix of direct and tortuous flow paths in DW.

additional flow paths into the soil and created flow channels, thereby increasing the hydraulic conductivity. Divya et al. (2018) also observed almost two orders of magnitude increase in saturated hydraulic conductivity of a clayey soil amended with polypropylene terephthalate (PPT) fibers at 0.5% by weight; from 3×10^{-8} cm/s to 1×10^{-6} cm/s. On the other hand, tortuosity may have increased due to excess (large volumes of) straw. In the current study, it is believed that adding more straw (DW1) caused the generation of more tortuous pathways, resulting in a decrease in hydraulic conductivity.

Sand amendment increased the hydraulic conductivity of the dredged material. DS5 had a hydraulic conductivity 3.5 times higher than that of D while 10% sand addition (DS10) improved the hydraulic conductivity of the dredged material by approximately 7 times. Increased sand content yielded a looser structure of the soil, and resulted in higher saturated hydraulic conductivity, consistent with the findings of

Fan et al. (2014). Sobti and Singh (2017) also obtained a positive correlation between saturated hydraulic conductivity and sand amendment.

Lastly, amending the dredged material with recycled glass aggregate showed similar improvements to hydraulic conductivity. DG5 had hydraulic conductivity of 8.9×10^{-5} cm/s, approximately 2.4 times higher than D. A larger increase in hydraulic conductivity was examined with DG10, which had a value 4.6 times that of the unamended dredged material. Amlashi et al. (2020) reported that replacing particles smaller than 5 mm standard granular base with recycled glass aggregate increased the porosity and increased saturated hydraulic conductivity. that the decrease in fine particles and increase in porosity causes and increase in hydraulic conductivity. Adding the coarse recycled glass aggregate to the dredged material provided similar benefits, due to changes in particle size and improvement of porosity.

Changes in hydraulic conductivity by coefficient of curvature (C_c) and coefficient of uniformity (C_u) are presented in Figure 11. C_u is a measure of how uniform and alike particles are to one another (Choo, 2020). Data indicates that higher C_c and C_u values yield higher saturated hydraulic conductivity values. Beyer (1964) method also indicated that C_u, along with the effective grain size (d_{10}), has direct effect on hydraulic conductivity.

Several empirical equations that utilize particle size uniformity, grain size, and porosity have been developed to estimate hydraulic conductivity (Kozeny-Carman, year 1927, Amer and Awad 1974, NAVFAC, 1974, Cabalar and Akbulut, 2016, Wang et al. 2018). Predictive capabilities of the three commonly used equations listed in Table 6 are presented in Figure 12. In most cases, the models overestimate the

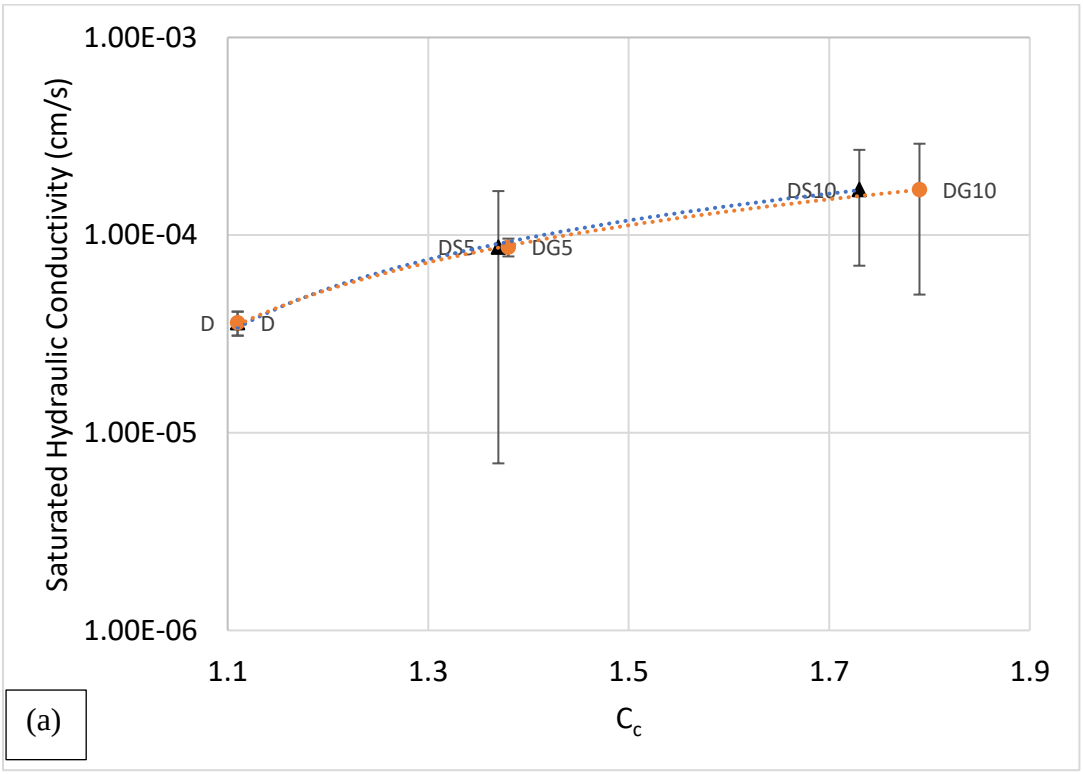

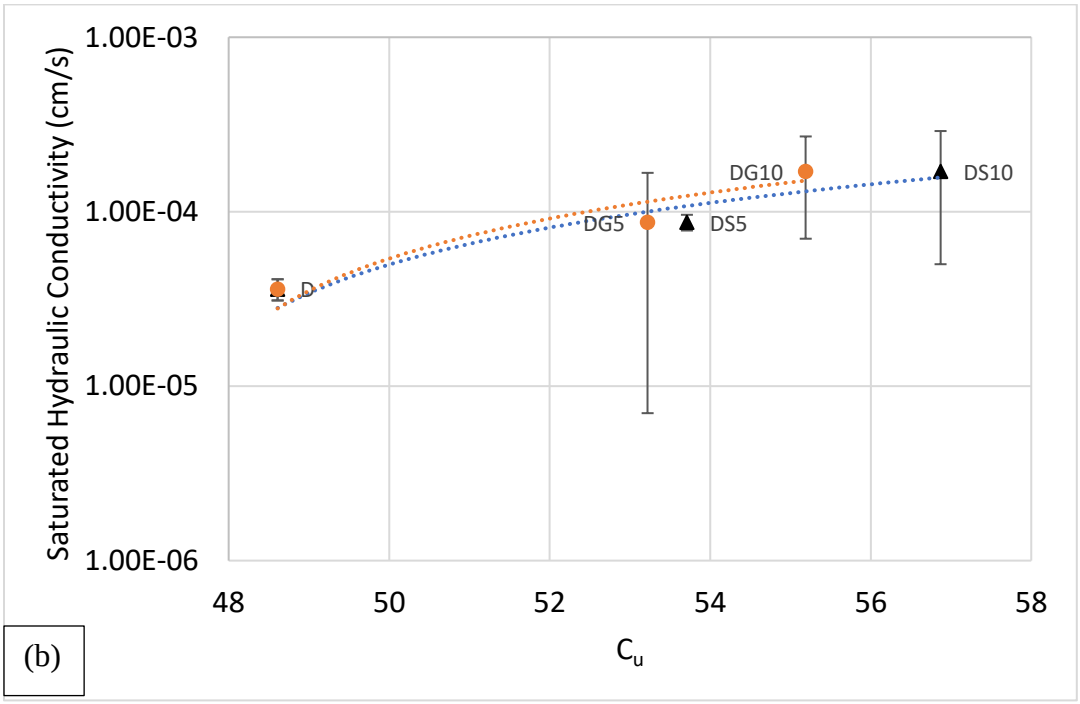

Figure 11. Changes in K_{sat} with (a) Cc and (b)Cu

Table 6. Empirical equation for hydraulic conductivity estimates

Researcher/Organization	Equation
Amer & Awad	$K = 35 * \left(\frac{e^3}{1+e}\right) * C_u^{0.6} * (d_{10})^{2.32}$
Kozeny-Carman	$K = 8.3 * 10^{-3} * \frac{g}{v} * \left[\frac{n^3}{(1-n)^2}\right] * (d_{10})^2$
NAVFAC	$K = 10^{1.291e-0.6435}(d_{10})10^{(0.5504-0.2937e)}$

Notes: *K= hydraulic conductivity (cm/s), e = void ratio, C_u = coefficient of uniformity, d_{10} = particle size coarser than 10%, n = porosity.*

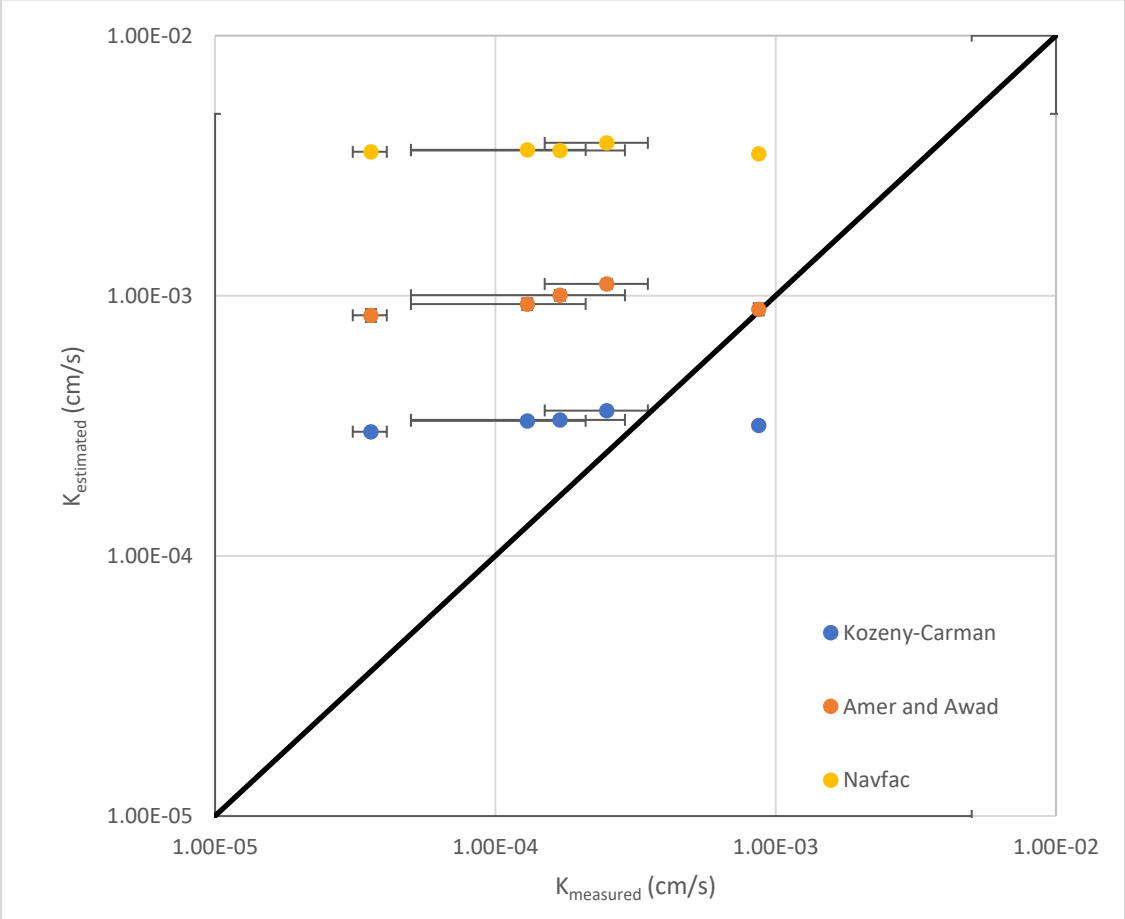

Figure 12. Comparison of laboratory measured K_{sat} values with those estimated through three empirical equations.

measured hydraulic conductivity, yielding unconservative estimated of infiltration times in designing such berms in practice.

3.2.2 Unsaturated Hydraulic Tests

Soil-water characteristics curves and their respective fitting parameters were obtained through the HYPROP Measurement System (HMS). Measurements of weight and matric suction made through this system were used to find the soil-water characteristics and hydraulic conductivity versus volumetric water content curves in Figures 13 and 14, respectively, by utilizing Equations 1 and 2.

During the development of soil-water characteristic curves, K_{sat} (saturated hydraulic conductivity) can be estimated as the hydraulic conductivity at saturated volumetric water content. Alternatively, saturated hydraulic conductivity values measured in the laboratory according to ASTM D5084 can be input into the HMS before applying the van Genuchten/Mualem models. Tables 7 and 8 provide a summary of the model parameters and the root mean square errors (RMSE) for the two methods. The RMSE represents the average discrepancy between the measured volumetric water content and the fitted curve (Pertassek et al., 2011). For instance, D has an RMSE of 0.0027, indicating an average disparity of 0.27% between the volumetric water content of data points and the fitted curve. Each material had duplicate tests, and of those, the ones that had a lower RMSE were selected. Models lacking predefined (lab measured) K_{sat} values exhibited comparatively lower RMSE values. In both scenarios, better fits (lower RMSE values) were observed for soil-water characteristic (retention) curves in comparison to unsaturated hydraulic conductivity-volumetric water content curves.

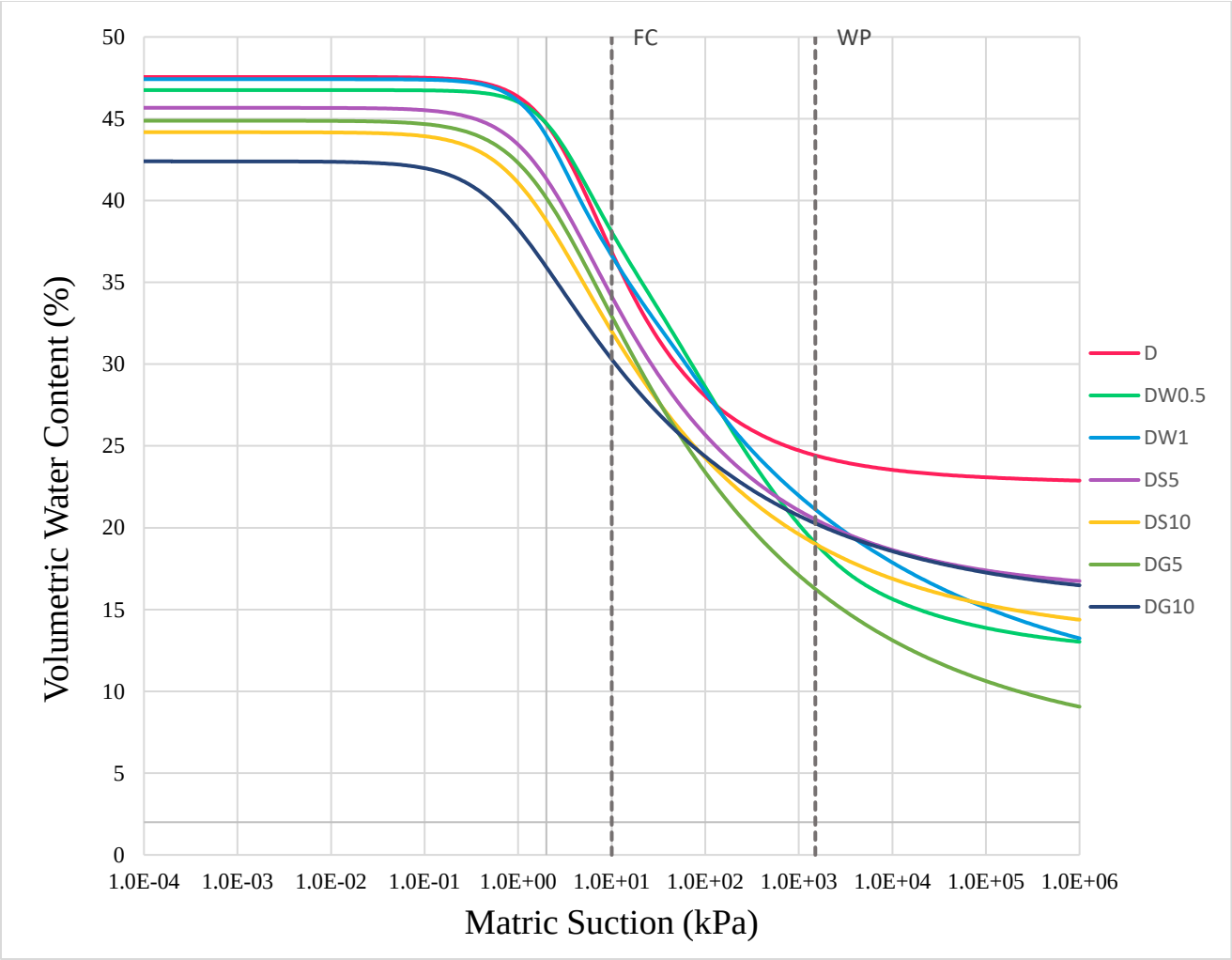

Figure 13. Soil-water characteristic curves of the materials tested.

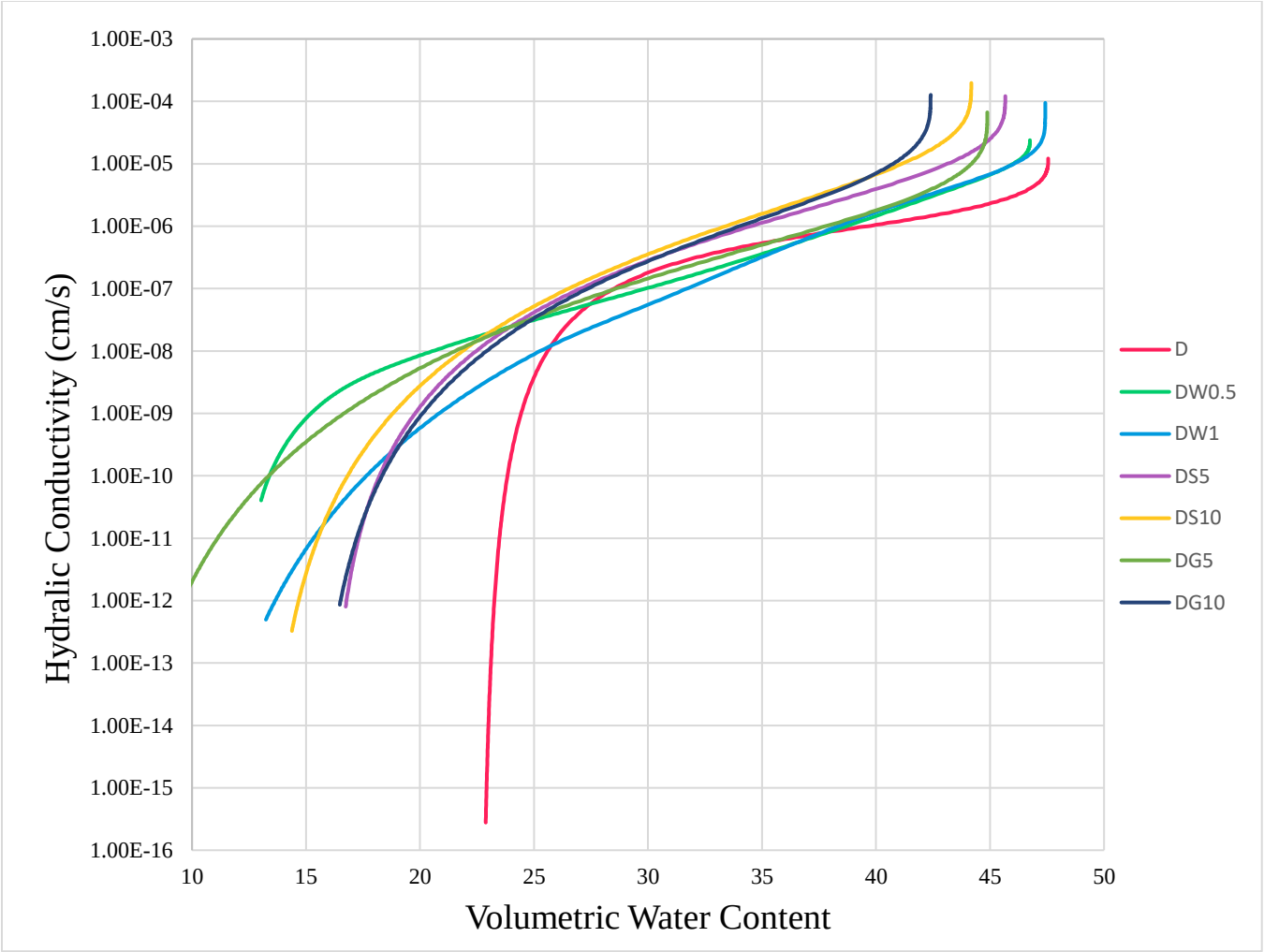

Figure 14. Hydraulic conductivity versus volumetric water content curves of the materials tested.

Table 7. Model parameters and RMSEs for van Genuchten constrained (1980) and van Genuchten/Mualem models by estimated K_{sat}

Material	θ_s (%)	θ_r (%)	n (-)	α (cm^{-1})	$K_{sat\ estimated}$ (cm/s)	τ (-)	RMSE (θ)	RMSE (K_{sat} estimated)
D	47.6	20.6	1.383	0.0320	1.8×10^{-5}	-5.13	0.0027	0.1376
DG5	45.7	1.7	1.154	0.0948	4.9×10^{-4}	<-6.00	0.0770	0.1845
DG10	41.9	18.6	1.329	0.0889	2.2×10^{-5}	-5.86	0.0053	0.1066
DW0.5	47.6	7.2	1.177	0.0344	2.7×10^{-4}	<-6.00	0.0481	0.1524
DW1	48.5	11.9	1.204	0.0569	2.0×10^{-4}	-5.39	0.0455	0.1750
DS5	45.6	16.4	1.291	0.0512	1.3×10^{-4}	-4.75	0.0321	0.1824
DS10	43.9	17.5	1.317	0.0657	1.1×10^{-4}	-4.52	0.0271	0.1605

Notes: θ_s: saturated volumetric water content, θ_r: residual water content, n: shape parameter related to bending of the retention curve, α: shape parameter [cm^{-1}] linked with the inverse of the air-entry pressure, $K_{sat\ estimated}$: saturated hydraulic conductivity estimated, τ: tortuosity parameter, RMSE (K_{sat} estimated): root mean squares error of van Genuchten/Mualem model, RMSE(θ): root mean squares error of van Genuchten (1980) model. Hyprop software reports tortuosities greater than 6.0 (i.e., <-6.0) as 6.0.

Table 8. Model parameters and RMSEs for van Genuchten constrained (1980) and van Genuchten /Mualem models using K_{sat} measured by ASTM D5084 procedure

Material	θ_s (%)	θ_r (%)	n (-)	α (cm^{-1})	K_{sat} (cm/s)	τ (-)	RMSE (θ)	RMSE (Ksat)
D	45.7	19.1	1.198	0.0489	3.7×10^{-5}	<-6.00	0.0039	0.1096
DG5	44.9	6.4	1.201	0.0575	8.9×10^{-5}	<-6.00	0.0182	0.0825
DG10	42.5	14.2	1.206	0.1476	1.7×10^{-4}	<-6.00	0.0554	0.1370
DW0.5	47.7	5.3	1.164	0.0358	3.6×10^{-4}	<-6.00	0.0482	0.1524
DW1	45.7	11.2	1.183	0.0458	6.4×10^{-5}	<-6.00	0.0455	0.1749
DS5	45.6	16.3	1.289	0.0513	1.3×10^{-4}	-4.75	0.0322	0.1838
DS10	44.2	13.1	1.235	0.0702	2.5×10^{-4}	-5.136	0.0552	0.1828

Notes: θ_s: saturated volumetric water content, θ_r: residual water content, n: shape parameter related to bending of the retention curve, α: shape parameter [cm^{-1}] linked with the inverse of the air-entry pressure, K_{sat}: saturated hydraulic conductivity measured in the laboratory, τ: tortuosity parameter, RMSE(K_{sat}): root mean squares error of van Genuchten/Mualem model, RMSE(θ): root mean squares error of van Genuchten (1980) model. Hyprop software reports tortuosities greater than 6.0 (i.e., <-6.0) as 6.0.

Field capacity (FC), wilting point (WP), and available water content (AWC) are provided in Table 8. These values are obtained from the functions based on the measured saturated hydraulic conductivity values and presented in Table 8. Organic matter (OM) significantly influences plant available water content (AWC) (Zibilske et al., 2000; Zare et al., 2010; Siahdashti et al., 2015). The data in Table 9 indicates an increase in available water content due to straw amendment. Similarly, Li et al. (2014) reported that treating silt loam soils with finely cut straw at 0.5% gravimetric content yields an increase in the volumetric water content at 10 kPa, which is the matric suction at field capacity. D has an AWC of 12.3% while DW0.5 and DW1 have AWC values of 18.8% and 15.4% respectively, showing an increase of 1.1.2-1.5 times by straw amendment, which can help with plant growth and erosion control (Gonzalez and Cooperband, 2002; Jennings et al., 2003; Kirchoff et al., 2003; Veeresh et al., 2003).

Smith (2024) conducted a mesocosm study in which he monitored the grass establishment of DW0.5, DW1, DS5 and D for a period of 71 days. The tests with the dredged sediments were performed in duplicate and named D1 and D2 (Figures A1 and A2 in Appendix). As seen in Figure A1, there is a change in rate of growth after ~30 days in all mesocosms, thus the growths at ay 30 and the final day (Day 71) were chosen for comparison. The relationships between the green cover and AWC at 30 days and 71 days are presented in Figure 15. If D2 is considered as an outlier, there is a strong correlation between AWC and green cover. While lab tests were conducted

Table 9. AWC, FC, WP and corresponding hydraulic conductivities.

	K_{FC} (cm/s)	K_{WP} (cm/s)	FC (%)	WP (%)	AWC (%)
D	2.53×10^{-7}	9.63×10^{-10}	36.7	24.4	12.3
DW0.5	2.17×10^{-7}	6.38×10^{-9}	37.9	19.1	18.8
DW1	1.14×10^{-7}	1.19×10^{-9}	36.5	21.1	15.4
DS5	2.11×10^{-7}	2.11×10^{-9}	34.0	20.5	13.5
DS10	1.42×10^{-7}	1.21×10^{-9}	31.9	19.0	12.9
DG5	7.14×10^{-8}	7.83×10^{-10}	32.8	16.3	16.5
DG10	7.83×10^{-8}	1.18×10^{-9}	30.2	20.3	9.9

Notes: K_{FC}: hydraulic conductivity at field capacity, K_{WP}: hydraulic conductivity at wilting point, FC: field capacity, WP: wilting point, AWC: available water content.

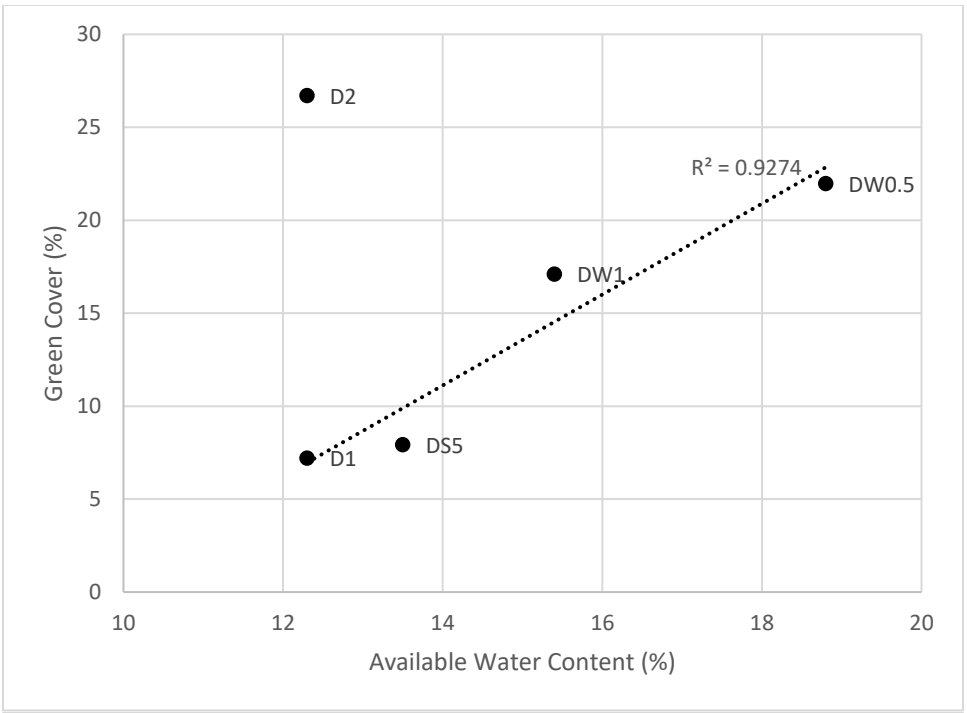

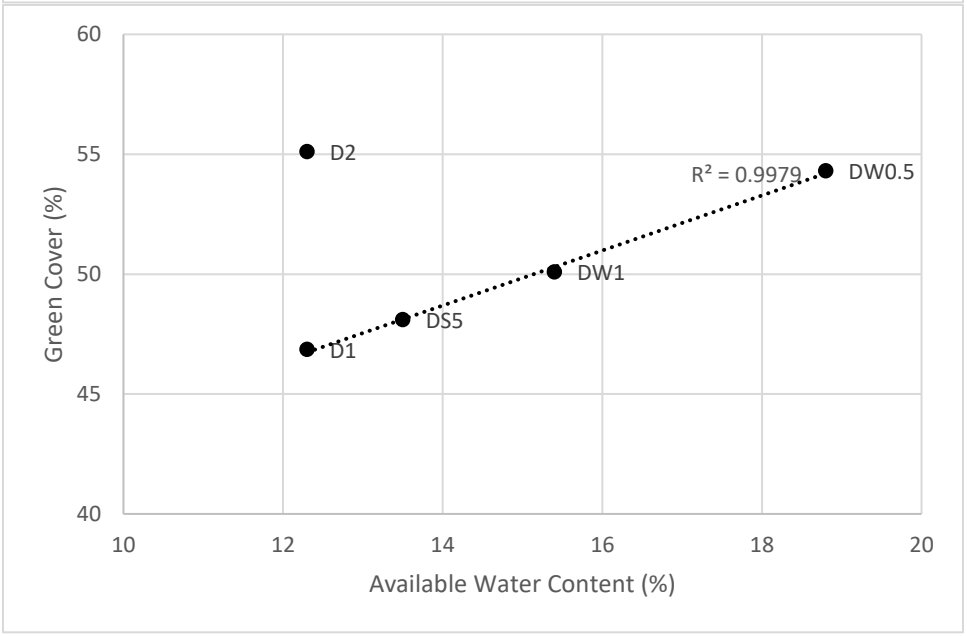

Figure 15. Green cover relationship with AWC at (a) 30 days, (b) 71 days. The trendlines exclude D2.

on specimens ≤ 4.75 mm in particle size, the mesocosm study did not discard any of these particles, which can be a reason for this discrepancy in behavior.

The information presented in Table 9 and Figure 16 indicates a noticeable decrease in unsaturated hydraulic conductivities of the materials tested, ranging from 1 to 3 orders of magnitude, as the values transition from field capacity (K_{FC}) to the wilting point (K_{WP}). Unamended dredged material, D, exhibits the highest drop, from 2.53×10^{-7} cm/s at field capacity to 9.63×10^{-10} cm/s at wilting point. DW0.5, which has a very comparable K_{FC} to D, has the highest K_{WP} at 6.38×10^{-9} cm/s. Hydraulic conductivity, as a function of saturation, utilizes the principle of water flowing through the water inside a soil specimen. Higher saturation, therefore higher volumetric water content, enables more pathways for water to flow through the soil. As drainage occurs, water takes up less space inside the pores, resulting in disconnected bodies of water that form films of water around solid particles. This increase in tortuosity reduces the hydraulic conductivity as the water now must travel through a longer path in the soil. According to Vereecken et al. (2010) the drop in unsaturated hydraulic conductivity is steeper with an increase in tortuosity. The steeper drop in DW1 as compared DW0.5 may be attributed to development of more tortuous pathways in specimens due to large volumes of straw (Figure 10).

At saturation, coarse grained soils, like DG10 and DS10, exhibit higher hydraulic conductivity due to their increased porosity compared to finer soils such as D. However, once the saturation values are lower (i.e., higher suction) finer soils (i.e., the dredged material, D) show higher hydraulic conductivity since the expulsion of water from smaller pores requires more matric suction which is attributed to the

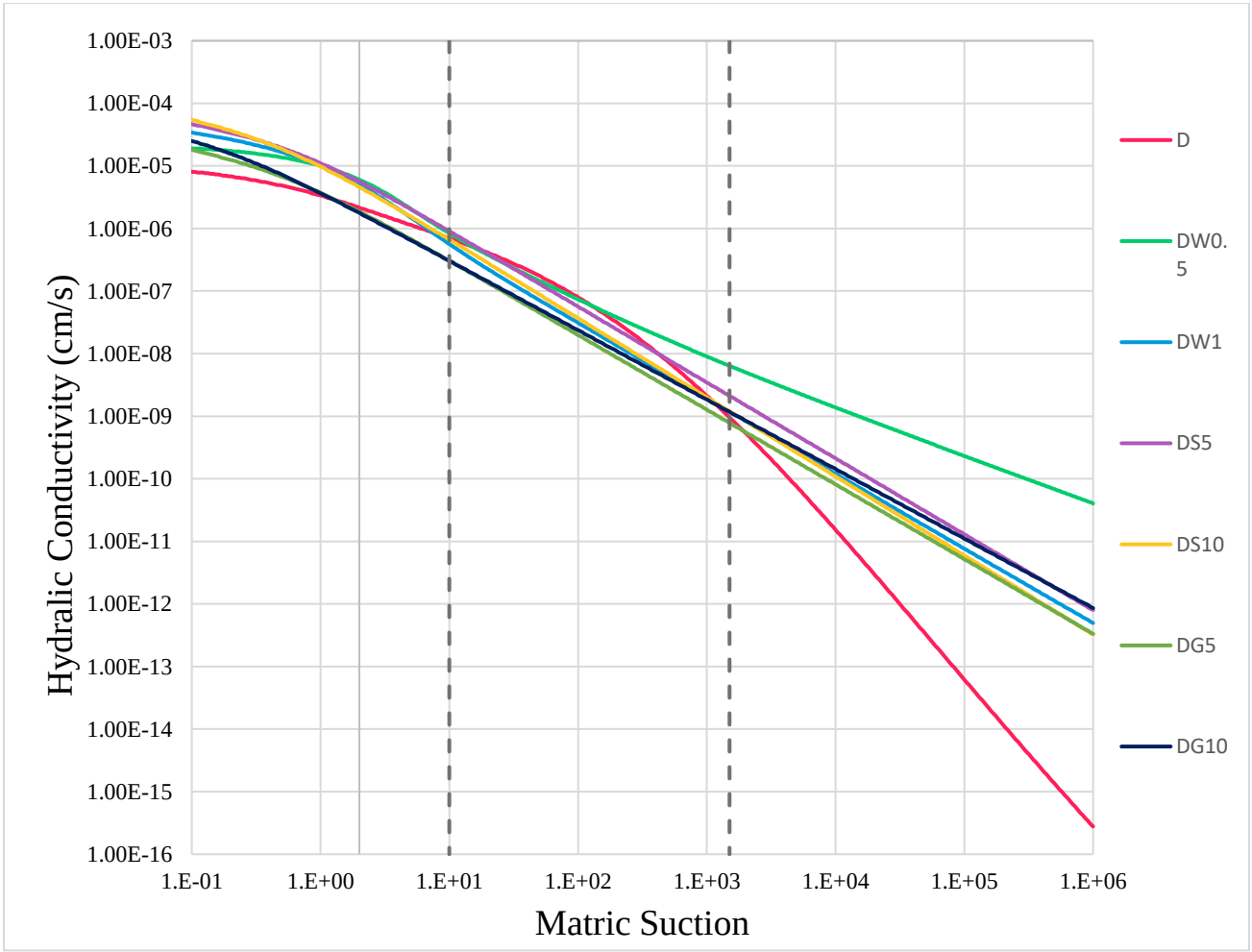

Figure 16. Hydraulic conductivities of materials at FC and WP

presence of a larger water film perimeter per unit cross-sectional area in soils with finer particles (Tokunaga, 2009).

3.3 Results of Numerical Modeling

3.3.1 Slope Stability Analysis

As VEBs are significantly smaller in size than common water containment and/or divergence structures, the design approach for slope stability was to examine the least desirable conditions. Initial modeling efforts in this study, supported by literature, showed that:

- Increasing the subgrade slope decreases the factor of safety (Figure 17a). Chatterjee and Krishna (2019) also expressed that stability of the slope decreased for silty sand and sandy silt soils used in analysis.
- Steep side slopes result in lower hydraulic conductivity values (Figure 17b), consistent with the findings of Shole and Belaney (2019) who showed that the reduction in the side slope of a dam makes the structure safer for slope stability.
- Increasing the subbase thickness can have a varying effect on slope stability (Figure 17c), depending on the soils used. The berm material and the subbase material considered in the current study have lower shear strength parameters as compared to Subgrade 1 and Subgrade 2, therefore, a thicker subbase layer results in lower factor of safety for slope stability, although it is not significant.

Considering these findings, the least desirable infiltration berm structure is the one with side slopes of 1H:1V, subgrade slope of 10H:1V and a subbase thickness of 0.62

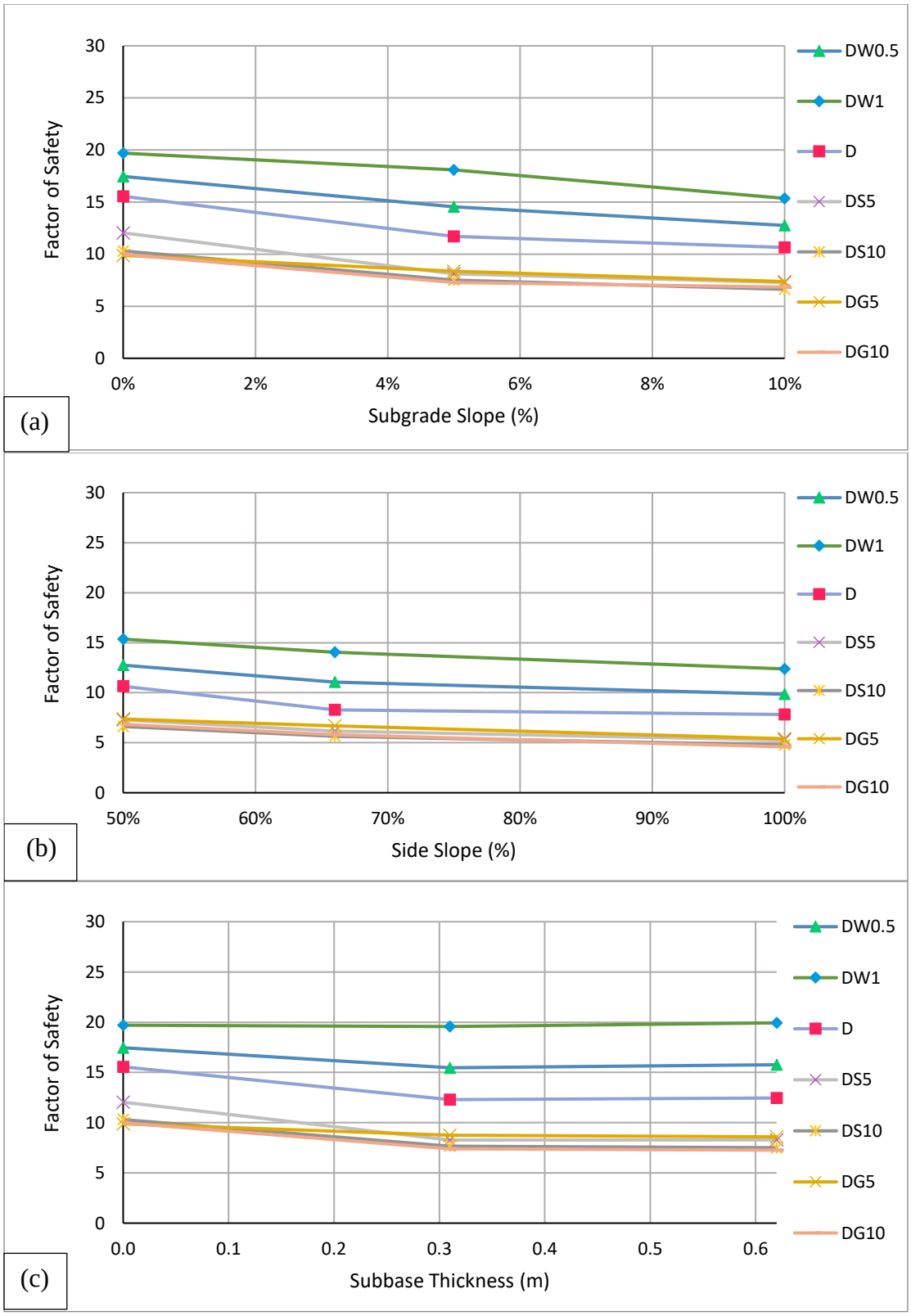

Figure 17. Change in factor of safety with respect to **(a)** subgrade slope, **(b)** side slope, and **(c)** subbase thickness.

meters, constructed with DG10. This design results in $FS_{downstream}$ of 4.59 which is significantly higher than FS_{design} of 1.4. As a result, no further attempts were made to numerically analyze additional scenarios.

3.3.1 Seepage Analysis

Influence of Berm Geometry on Infiltration

As the subbase becomes thicker, time for complete infiltration reduces. For example, Figure 18a shows how the required time for infiltration changes with subbase thickness for berm with a side slope of 2H:1V constructed on a subgrade slope of 10H:1V. As the berm materials used in analyses all have higher hydraulic conductivity values than the common subgrade materials, Subgrade 1 and Subgrade 2, the utilization of more dredged material in subbase layer construction reduces the infiltration time. Because most of the berm materials with no subbase failed to provide total infiltration under 72 hours (3 days), remaining analyses focused on designs with subbases thickness of 0.31 m and 0.62 m.

Subgrade slope has a similar effect on time for full infiltration. Time-to-infiltrate reduces significantly as the subgrade slope is increased (Figure 18b). Increasing the subgrade slope causes the hydraulic gradient to increase, resulting in increased flow velocity through the infiltration berm.

Lastly, changing the side slope also has a similar effect on times required for full infiltration. Figure 18c shows the results for an infiltration berm constructed on a 0.62-m thick subbase and a subgrade with a slope of 10H:1V. Increasing the slope of

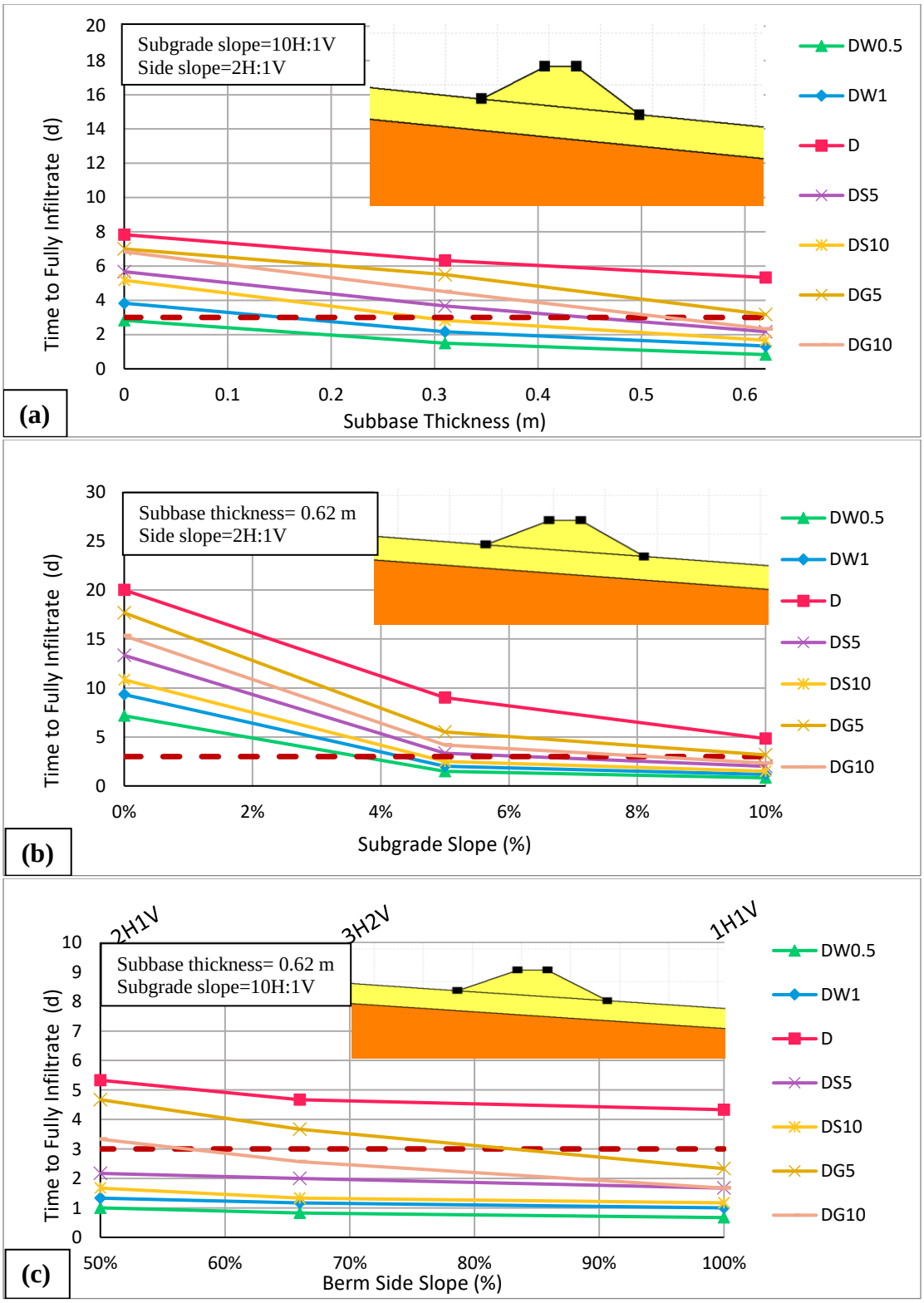

Figure 18. Time-to-fully infiltrate versus **(a)** subbase thickness, **(b)** subgrade slope, and **(c)** side slope for berms constructed with different materials. Berm height is 0.62 m, crest width is 0.62 m, and impounded water height is 0.62 m. The dashed line represents the infiltration time limit of 3 days.

the berm reduces the time required for infiltration. Although there is a positive correlation, it is not as pronounced as the effects of the subgrade slope with regards to infiltration time.

For all designs proposed, straw-amended dredged materials yield the shortest infiltration times, and the order is DW0.5<DW1< DS10<DS5<DG10<DG10<D. The dredged material (D) fails to provide infiltration in the required time span of 3 days across all designs, making the requirement to amend it apparent.

Influence of Berm Geometry on Piping

As seen in Figure 19a, increasing the berm side slope results in a lower FS_{piping} across all soils. O'Shaughnessy et al. (2023) reported that, among 3 different embankment side slopes tested, the steepest side slope of 2H:1V resulted in the lowest FS_{piping} while the gentlest slope of 6H:1V yielded the safest design with regards to piping failure. As none of the berms modeled with 3H:1V and 1H:1V side slopes produced sufficient factors of safety, the remainder of the piping analyses focused on berms with 2H:1V side slopes.

The subgrade slope has an inconsistent effect on FS_{piping}. For all soils, a subgrade slope of 5% makes the design less safe while an increased subgrade slope of 10% makes the design safer against piping by increasing FS_{piping} (Figure 19b). The subbase thickness and its effects on piping are presented in Figure 19c. The thickness of the subbase provides unnoticeable changes that do not affect the safety of berms against a piping failure.

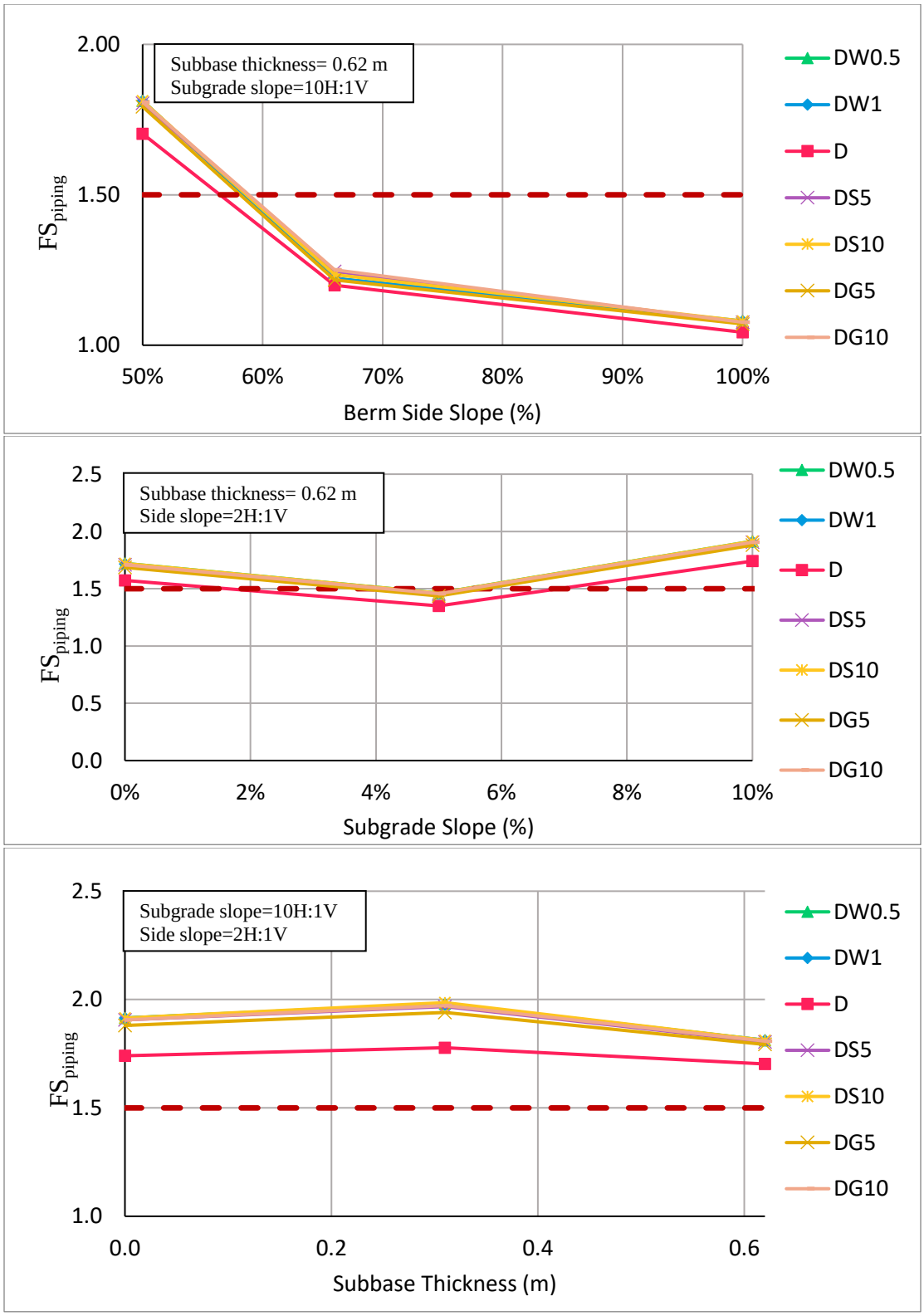

Figure 19. Effect of **(a)** berm side slope, **(b)** subgrade slope, and **(c)** subbase thickness on FS_{piping} for berms constructed with different materials. Berm height is 0.62 m, crest width is 0.62 m, and impounded water height is 0.62 m. The dashed line represents design FS_{piping}.

Initial analysis showed that presence of Subgrade 1 or Subgrade 2, did not influence the infiltration times significantly (not shown herein). For that reason, a reverse approach was followed to back calculate the minimum subgrade hydraulic conductivities required to have an infiltration time of 3 days for the berms. Since presence of a subbase decreases infiltration times (Figure 18a) and does not significantly influence the factor of safety against piping (Figure 19c), no subbase was assumed to exist. The findings presented in Table 10 can be of use to practitioners for an initial estimate for a successful design. However, it is strongly recommended to back up these initial calculations with laboratory and field tests before full-scale field implementation.

Table 10. Minimum subgrade hydraulic conductivities (cm/s) required to have an infiltration time of 3 days for the berms. No subbase is assumed to exist.

Berm Material	Side Slope 2H:1V			Side Slope 3H:2V			Side Slope 1H:1V		
	Subgrade Slope 10H:1V	Subgrade Slope 20H:1V	No Subgrade Slope	Subgrade Slope 10H:1V	Subgrade Slope 20H:1V	No Subgrade Slope	Subgrade Slope 10H:1V	Subgrade Slope 20H:1V	No Subgrade Slope
D	1.5×10^{-5}	2.5×10^{-5}	1.1×10^{-3}	1.2×10^{-5}	2.3×10^{-5}	9.5×10^{-4}	1.0×10^{-5}	2.0×10^{-5}	8.7×10^{-4}
DS5	3.4×10^{-5}	5.0×10^{-5}	9.4×10^{-4}	2.5×10^{-5}	4.1×10^{-5}	8.4×10^{-4}	1.9×10^{-5}	3.8×10^{-5}	7.8×10^{-4}
DS10	3.0×10^{-5}	4.7×10^{-5}	8.2×10^{-4}	2.3×10^{-5}	4.0×10^{-5}	7.9×10^{-4}	1.8×10^{-5}	3.6×10^{-5}	7.0×10^{-4}
DG5	2.7×10^{-5}	4.4×10^{-5}	8.9×10^{-4}	2.5×10^{-5}	3.9×10^{-5}	8.3×10^{-4}	1.8×10^{-5}	3.5×10^{-5}	7.6×10^{-4}
DG10	3.2×10^{-5}	4.7×10^{-5}	9.2×10^{-4}	2.8×10^{-5}	4.4×10^{-5}	8.8×10^{-4}	2.0×10^{-5}	4.0×10^{-5}	8.0×10^{-4}
DW0.5	1.3×10^{-5}	2.6×10^{-5}	8.5×10^{-4}	1.0×10^{-6}	2.4×10^{-5}	8.0×10^{-4}	7.1×10^{-6}	2.2×10^{-5}	7.5×10^{-4}
DW1	1.4×10^{-5}	3.7×10^{-5}	9.5×10^{-4}	9.7×10^{-6}	2.8×10^{-5}	8.9×10^{-4}	7.4×10^{-6}	2.1×10^{-5}	8.2×10^{-4}

Notes: Side Slope: Slope of the berm, Subgrade Slope: Slope of the surface the berm is constructed on, H:V: Ratio of the horizontal and vertical components of slope.

Chapter 4

Conclusions

4.1 Summary and Conclusions

A research study was undertaken to define geotechnical properties of Baltimore dredged material and its amended blends for their possible use in construction of a vegetated infiltration berm. Unconfined compression tests were performed to identify the shear strength properties of the materials. Stability analyses of berms with varying geometries were performed by utilizing the laboratory-measured shear strength properties. Bubble-tube permeameters and HYPROP system were used to perform saturated and unsaturated hydraulic conductivity tests, respectively, on the materials. The results of these hydraulic tests were then used to numerically model seepage through the berms. The following conclusions were made:

1) Undrained cohesion of the dredged material (14.8 kPa) increased 1.8- 2.5 times with wheat straw amendment (53-36.7 kPa). Undrained cohesion of dredged material (D) dropped when amended with 5% sand (13.1 kPa), 10% sand (11.9 kPa), 5% recycled glass aggregate (13.5 kPa) and 10% recycled glass aggregate (11.5 kPa); all amendments were added by weight.
2) Saturated hydraulic conductivity (K_{sat}) of the dredged material increased from 3.7×10^{-5} cm/s to $1.3\text{-}2.5 \times 10^{-4}$ cm/s because of sand amendment. Recycled glass aggregate amendment at 5% (8.9×10^{-5} cm/s) and 10% (1.7×10^{-4} cm/s) increased saturated hydraulic conductivity 2.4 to 4.6 times while straw

amendment effect dipped after adding the straw at 1% (6.4×10^{-5} cm/s) as compared to 0.5% (3.6×10^{-4} cm/s).

3) Dredged material had a plant available water content (AWC) of 6.9%. Wheat straw amendments at 5 % and 10% increased the AWC of dredged material by 1.6-2 times, increasing the potential of plant growth on the infiltration berms. These amendments also reduced the rate of decrease in unsaturated hydraulic conductivity as matric suction increases, due to formation of a coarser material. The dredged material (D) had a hydraulic conductivity of 9.6×10^{-10} cm/s at wilting point (WP) whereas DW0.5 and DW1 had hydraulic conductivities of 6.4×10^{-9} cm/s and 1.19×10^{-9} cm/s, respectively, providing more water flow in a drier range. Hydraulic conductivities of all soil blends were comparable at field capacity (FC) except the specimens prepared with recycled glass aggregate; their hydraulic conductivities were 4 times lower than that of D.
4) All berm designs considered in this study, including all geometries and soils, satisfied the proposed factor of safety against rotational failure. FS values were greater than 4.6, indicating that a stability analysis would not be required in designing these shallow systems.
5) When infiltration time is considered, a steeper subgrade slope along with a steeper berm side slope and thicker subbase are desirable as all three changes result in significantly reduced infiltration times.
6) Subbase thickness does not have a significant impact on piping effect whereas increasing berm side slope greatly reduces FS_{piping}. 5% subgrade slope should be avoided whereas 10% is safe for the proposed design.

7) Unamended dredged material does not provide infiltration in the allotted time frame (3 days) and thus it needs to be either amended with straw or the berm should be placed on a subgrade soil that is hydraulically more conductive than Subgrade 1 and Subgrade 2.

4.2 Design Suggestions & Limitations

Suggestions for Amended Berm

- An infiltration berm should always be constructed on a subgrade slope. If a subgrade slope does not exist in the proposed area of application, a slope of 10% should be introduced to help satisfy the design. Steeper side slopes can also be eligible for such design, given they are modeled and analyzed first.
- To satisfy the safety criteria against piping failure, the berm should not have a side slope steeper than 50% (2H:1V) as any steeper side slope failed to meet the criteria for the conditions considered in the current study.
- As the introduction of a subbase provides additional infiltration to the design, subbases, preferably with straw amended dredged material, should be applied as thick of a layer as possible. Note that the design was analyzed for up to 0.62-meter-thick subbase, any subbase thicker should be reanalyzed to check for the other criteria.
- If a berm is to be constructed on native Maryland subgrade soil, Subgrade 1 or 2, amending a clayey sand (SC) dredged material with wheat straw at 0.5% percent by weight (DW0.5) is likely to yield the best results. This blend provided adequate hydraulic conductivity, met the required minimum

infiltration times, and acceptable AWC to promote vegetation, without experiencing any slope stability problems or piping failures (Figure 20).

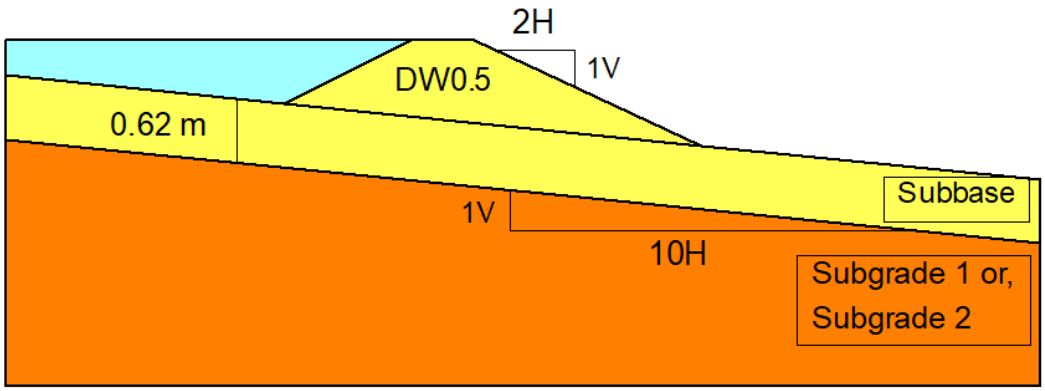

Figure 20: Proposed berm design

Suggestions for Unamended Berm

- Construction on subgrade soils more hydraulically conductive than those considered in this study (i.e., Eastern shore) may not require any dredge material stabilization. The same construction may also not require any subgrade slope, if the subgrade meets the minimum hydraulic conductivity requirements (Table 10).
- A more detailed look into wheat straw amendment through examination of different amendment percentages and different wheat straw lengths is advised to optimize the benefits of this amendment.

Limitations

- One key limitation of the study is the variation of dredged material samples obtained from the site. The material was collected in buckets and hauled to the Whiting-Turner Infrastructure Engineering Laboratories at the University of Maryland, College Park. Due to heterogeneous nature of the material, particle

size distributions varied from one bucket to another. In order to minimize this heterogeneity, the materials in the buckets were mixed before testing, which may be impractical in a field application.

- The dredged material was stockpiled in the field site without any cap. This may have resulted in the loss of some of the fines in certain parts of the stockpile due to wind and other climatic stresses. The percentage of fines varied among samples collected at different times (i.e., summer and winter). To minimize changes in fines content, enough material for testing (e.g., 100 buckets in our study) needs to be hauled in one single shipment.

Appendix

Figure A1. Logistic regression fits with green cover data points with σ parameter indicated, dashed vertical line (from Smith, 2024)

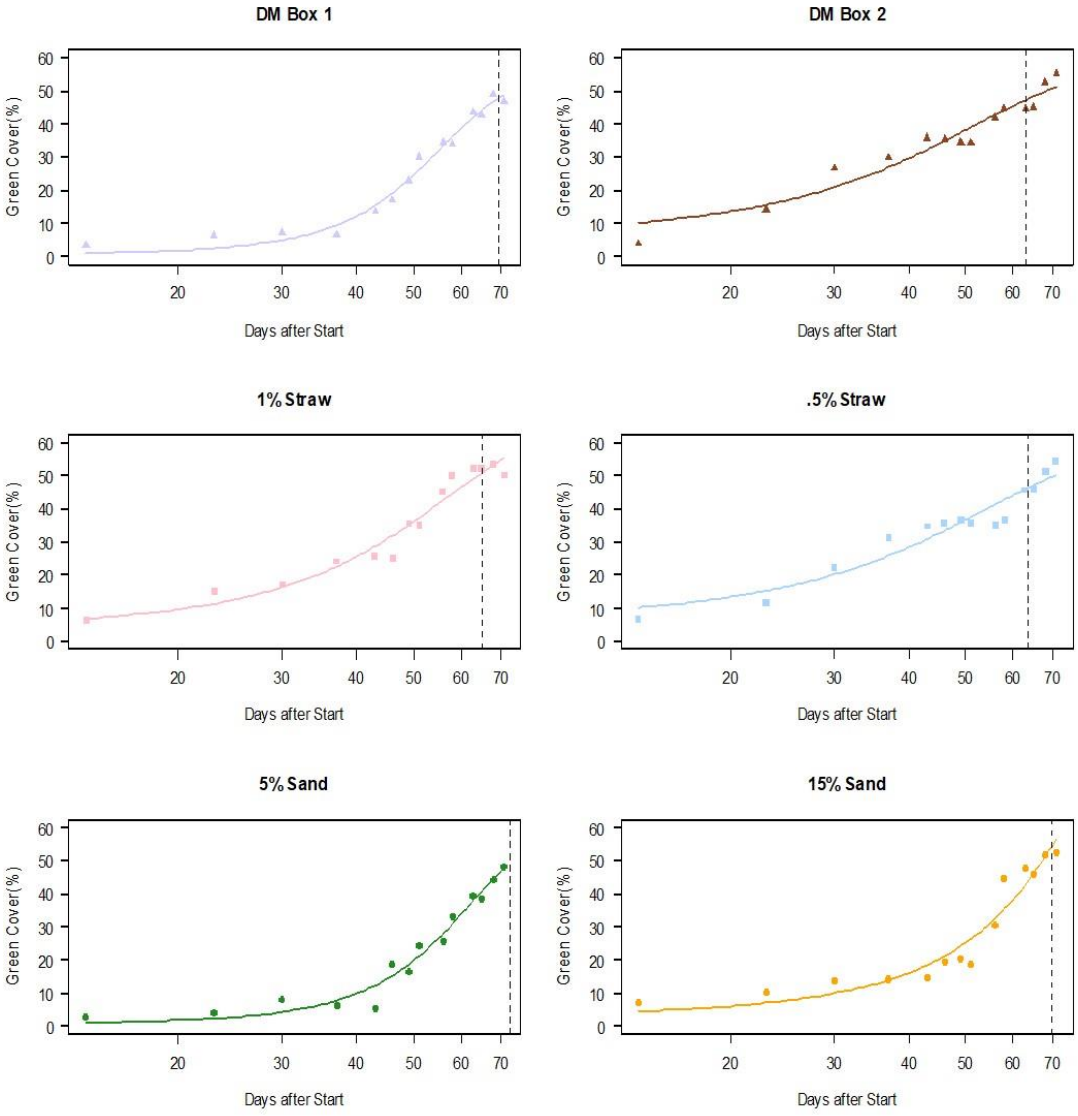

Figure A2. Green cover in the mesocosm boxes tracked with the elapsed time since the start of the mesocosm study; standard error (2%) of Canopeo green cover shown with error bars (from Smith, 2024).

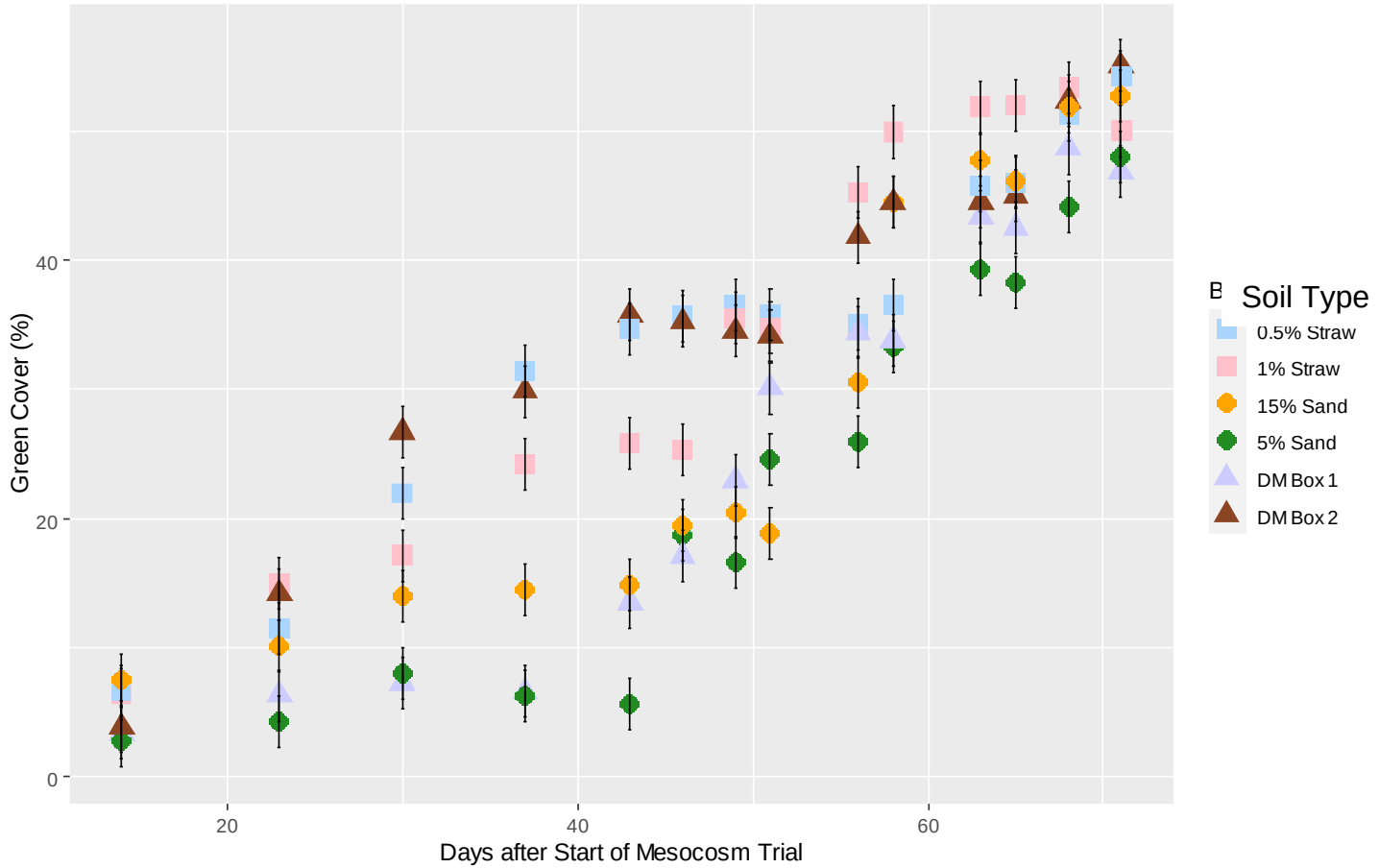

Table A1. Technical Release 210-60 Earth Dams and Reservoirs,Figure 5–3: Table of Static Slope Stability Criteria (from USDA NRCS, 2019)

Design condition	Primary assumption	Remarks	Applicable shear strength parameters	Minimum safety factor
1. Construction Stability (upstream or downstream slope)	Zones of the embankment or layers of the foundation expected to develop significant pore pressures during construction	Low-permeability embankment soils should be tested at water contents that are as wet as likely during construction (usually wet of optimum). Saturated low permeable foundation soils not expected to consolidate fully during construction. Existing dams with additional fill placed above saturated low-permeability zones.	Unconsolidated; Total stress consistent with preconstruction stress state	1.4 for failure surfaces extending into foundation layers 1.3 for embankments on stronger foundations where the failure surface is located entirely in the embankment
	Embankment zones and/or strata not expected to develop significant pore pressures during construction	Embankment zones, foundation strata, or both comprised of material with a permeability high enough to drain as rapidly as they are loaded	Effective stress	
2. Rapid drawdown (upstream slope)	Drawdown from the highest normal pool to the lowest gated outlet	Consider failure surfaces both within the embankment and extending into the foundation Low-permeability embankment and foundation soils that will have limited drainage during reservoir drawdown	Lowest of effective stress or consolidated; total stress; consistent with predrawdown consolidation stresses (See fig. 5-1)	1.2 1.1 for near surface (infinite slope) failure surfaces in cohesionless soils
		Embankment zones, foundation strata, or both comprised of material with a permeability high enough to drain as the reservoir is drawn down	Effective stress	
3. Steady seepage	Reservoir water surface at highest normal pool. Phreatic surface developed from the highest normal pool; typically the principal spillway crest	Consider failure surfaces within both the embankment and extending into the foundation. Foundation analysis may require separate phreatic surface evaluation, particularly in sites with confined seepage that results in uplift at the downstream toe.	Effective stress	1.5 1.3 for near surface (infinite slope) failure surfaces in cohesionless soils
4. Flood surcharge	Reservoir at freeboard hydrograph level. Steady seepage phreatic surface incorporating increased pore water pressure that may occur from flood detention and pore water pressure from short term seepage resulting from reservoir surface above the normal pool elevation	Consider failure surfaces within both the embankment and extending into the foundation. Embankment zones, foundation strata, or both comprised of material with a permeability high enough to drain rapidly with changes in reservoir elevation	Effective stress	1.4 1.2 for near surface (infinite slope) failure surfaces in cohesionless soils
		Low-permeability embankment and foundation soils that will have limited drainage as the increased reservoir load is applied	Lowest of effective stress or consolidated; total stress (See fig. 5-1)	

References

Alkroosh, I., Al-Robay, A., Sarker, P., & Alzabeebee, S. (2021). Effect of Sand Percentage on the Compaction Properties and Undrained Shear Strength of Low Plasticity Clay. In ARO-the Scientific Journal of Koya University (Vol. 9, Issue 1, pp. 16–20). Koya University. https://doi.org/10.14500/aro.10748

Amer, A. M., & Awad, A. A. (1974). Permeability of Cohesionless Soils. In Journal of the Geotechnical Engineering Division (Vol. 100, Issue 12, pp. 1309–1316). American Society of Civil Engineers (ASCE). https://doi.org/10.1061/ajgeb6.0000134

Amiri, S. T. (2018). Experimental study of geotechnical characteristics of crushed glass mixed with kaolinite soil. In International Journal of GEOMATE (Vol. 14, Issue 45). International Journal of Geomate. https://doi.org/10.21660/2018.45.83839

ASTM International. 2021. *Standard Test* Methods for Laboratory Determination of Water (Moisture) Content of Soil and Rock by Mass. ASTM International. https://doi.org/10.1520/d2216-19

ASTM International. 2021. *Standard Test* Methods for Liquid Limit, Plastic Limit, and Plasticity Index of Soils. ASTM International. https://doi.org/10.1520/d4318-17e01

ASTM International. 2021. *Standard Test* Method for Permeability of Granular Soils (Constant Head). ASTM International. https://doi.org/10.1520/d2434-19

ASTM International. 2021. *Standard* Test Methods for Sieve Analysis and Water Content of Refractory Materials. ASTM International. https://doi.org/10.1520/c0092-95r22e01

ASTM International. 2021. *Standard* Test Method for Unconfined Compressive Strength of Cohesive Soil. ASTM International. https://doi.org/10.1520/d2166-06

Briaud, J.-L., L. Maddah, National Research Council (US) Transportation Research Board, National Cooperative Highway Research Program, American Association of State Highway and Transportation Officials, and US Federal Highway Administration. 2016. Minimizing roadway embankment damage from flooding (NCHRP synthesis, no. 496). Washington, DC: Transportation Research Board.

Cabalar, A. F., & Akbulut, N. (2016). Evaluation of actual and estimated hydraulic conductivity of sands with different gradation and shape. In SpringerPlus

(Vol. 5, Issue 1). Springer Science and Business Media LLC. https://doi.org/10.1186/s40064-016-2472-2

Carman PC (1956) Flow of gases through porous media. Butterworths Scientific Publications, London

Chatterjee, D., & Murali Krishna, A. (2019). Effect of Slope Angle on the Stability of a Slope Under Rainfall Infiltration. In Indian Geotechnical Journal (Vol. 49, Issue 6, pp. 708–717). Springer Science and Business Media LLC. https://doi.org/10.1007/s40098-019-00362-w

Choo, H., Zhao, Q., Burns, S. E., Sturm, T. W., & Hong, S. H. (2020). Laboratory and theoretical evaluation of impact of packing density, particle shape, and uniformity coefficient on erodibility of coarse-grained soil particles. In Earth Surface Processes and Landforms (Vol. 45, Issue 7, pp. 1499–1509). Wiley. https://doi.org/10.1002/esp.4825

Colman, E. A. 1947. "A laboratory procedure for determining the field capacity of field soils." *Soil Sci.* 63: 277-283.

Dayioglu, A. Y., & Aydilek, A. H. (2019). Effect of pH and Subgrade Type on Trace-Metal Leaching from Steel-Slag Embankments into Groundwater. In Journal of Materials in Civil Engineering (Vol. 31, Issue 8). American Society of Civil Engineers (ASCE). https://doi.org/10.1061/(asce)mt.1943-5533.0002777

Divya, P. V., Viswanadham, B. V. S., & Gourc, J. P. (2018). Hydraulic conductivity behaviour of soil blended with geofiber inclusions. In Geotextiles and Geomembranes (Vol. 46, Issue 2, pp. 121–130). Elsevier BV. https://doi.org/10.1016/j.geotexmem.2017.10.008

Fang, H., Zhang, Q., Ji, C., & Guo, J. (2016). Soil shear properties as influenced by straw content: An evaluation of field-collected and laboratory-remolded soils. In Journal of Integrative Agriculture (Vol. 15, Issue 12, pp. 2848–2854). Elsevier BV. https://doi.org/10.1016/s2095-3119(15)61327-2

Francingues, N. R., Thompson, D. W., Hamons, F. L. (2011) Exploring innovative reuse of dredged material from Baltimore harbor. *Proceedings of 2011 WEDA Technical Conference and Texas A&M Dredging Seminar*, Nashville, Tennessee, June 5-8, 2011.

Geo-Slope International. 2012. "Seepage Modeling with SEEP/W." Accessed May 6, 2024. http://downloads.geoslope. com/geostudioresources/8/0/6/books/seep%20modeling.pdf?v=8.0.7.6129.

Gonzalez, R. F., and Cooperband, L. R. 2002. “Compost effects on soil physical properties and field nursery production.” *Compost Science & Utilization* 10: 226–237. https://doi.org/10.1080/1065657X.2002.10702084.

Houlihan, M., Bilgen, G., Dayioglu, A. Y., & Aydilek, A. H. (2021). Geoenvironmental Evaluation of RCA-Stabilized Dredged Marine Sediments as Embankment Material. In Journal of Materials in Civil Engineering (Vol. 33, Issue 1). American Society of Civil Engineers (ASCE). https://doi.org/10.1061/(asce)mt.1943-5533.0003547

Huntington, T. G. 2007. “Available water capacity and soil organic matter.” *Encyclopedia of soil science. New York: Taylor and Francis* 139–143.

Jamison, V. C., and E. M. Kroth. 1958. “Available moisture storage capacity in relation to textural composition and organic matter content of several Missouri Soils1.” *Soil Sci. Soc. Am. J.* 22 (3): 189-192. https://doi.org/10.2136/sssaj1958.03615995002200030001x.

Jennings, S. R., J. D. Goering, P. S. Blicker, and J. J. Taverna. 2003. “Evaluation of organic matter addition and incorporation on steep cut slopes phase I: Literature review and potential application equipment evaluation.” Montana Department of Transportation Research Program, Helena MT.

Joyce, J. M., & Scott, S. M., An Assessment of Maryland’s Vulnerability to Flood Damage. Baltimore (MD): Maryland Department of the Environment (US); August 2005

Khan, F. S., Azam, S., Raghunandan, M. E., & Clark, R. (2014). Compressive Strength of Compacted Clay-Sand Mixes. In Advances in Materials Science and Engineering (Vol. 2014, pp. 1–6). Hindawi Limited. https://doi.org/10.1155/2014/921815

Kirchoff, C., Malina, J., and Barrett, M. 2003. “Characteristics of compost: moisture holding and water quality improvement.” *Center for Research in Water Resources.* 1-4.

Kirkham, M. B. 2005. “Principles of soil and plant water relations.” *Burlington: Academic Press* 500.

Kozeny J (1927) Uber Kapillare Leitung Des Wassers in Boden. Sitzungsber Akad. Wiss.Wien Math.Naturwiss.Kl., Abt.2a, 136:271–306 (in German)

Li et al. (2014) Effect of Straw Pretreatment on the Soil Water-Holding Capacity and Evaporation in Low-Suction Section. In Nature Environment and Pollution Technology (Vol. 13, No. 3, pp. 565-570). https://neptjournal.com/upload-images/NL-49-21-(19)D-78Com.pdf

Li, M., Xi Chai, S., Yuan Zhang, H., Pu Du, H., & Wei, L. (2012). Feasibility of saline soil reinforced with treated wheat straw and lime. In Soils and Foundations (Vol. 52, Issue 2, pp. 228–238). Elsevier BV. https://doi.org/10.1016/j.sandf.2012.02.003

Malasavage, N. E., Jagupilla, S., Grubb, D. G., Wazne, M., & Coon, W. P. (2012). Geotechnical Performance of Dredged Material—Steel Slag Fines Blends: Laboratory and Field Evaluation. In Journal of Geotechnical and Geoenvironmental Engineering (Vol. 138, Issue 8, pp. 981–991). American Society of Civil Engineers (ASCE). https://doi.org/10.1061/(asce)gt.1943-5606.0000658

Minasny, B., and McBratney, A. B. 2018. "Limited effect of organic matter on soil available water capacity." *Eur. J. Soil Sci.* 69: 39–47. https://doi.org/10.1111/ejss.12475.

Mohsenian Hadad Amlashi, S., Carter, A., Vaillancourt, M., & Bilodeau, J.-P. (2020). Physical and hydraulic properties of recycled glass as granular materials for pavement structure. In Canadian Journal of Civil Engineering (Vol. 47, Issue 7, pp. 865–874). Canadian Science Publishing. https://doi.org/10.1139/cjce-2019-0089

NAVFAC (Naval Facilities Engineering Command) (1974) Soil mechanics, foundations, and earth structures. Design manual DM7. US Government Printing Office, Washington, DC

NRCS (2019). *Soil Health – Bulk Density/Moisture/Aeration.* Guides for Educators

NRCS. 2019. "Technical Release 210-60 Earth Dams and Reservoirs." Accessed June 14, 2022. https://directives.sc.egov.usda.gov/OpenNonWebContent.aspx?content=43317.wba.

O'Shaughnessy, A., Dayioglu, A. Y., Davis, A. P., & Aydilek, A. H. (2023). When roads want to be dams: looking to dam safety to regulate transportation embankments. In Natural Hazards (Vol. 120, Issue 3, pp. 2349–2378). Springer Science and Business Media LLC. https://doi.org/10.1007/s11069-023-06270-w

Ratliff, L. F., J. T. Ritchie, and D. K. Cassel. 1983. "Field-measured limits of soil water availability as related to laboratory-measured properties1." *Soil Sci. Soc. Am. J.* 47: 770-775. https://doi.org/10.2136/sssaj1983.03615995004700040032x.

Rosas, J., Lopez, O., Missimer, T. M., Coulibaly, K. M., Dehwah, A. H. A., Sesler, K., Lujan, L. R., & Mantilla, D. (2013). Determination of Hydraulic

Conductivity from Grain-Size Distribution for Different Depositional Environments. In Groundwater (Vol. 52, Issue 3, pp. 399–413). Wiley. https://doi.org/10.1111/gwat.12078

Satyanaga, A., Abishev, R., Sharipov, A., Wijaya, M., Hamdany, A. H., Moon, S.-W., & Kim, J. (2023). Effect of slope geometry on stability of slope in Almaty. In M. Bardanis (Ed.), E3S Web of Conferences (Vol. 382, p. 13005). EDP Sciences. https://doi.org/10.1051/e3sconf/202338213005

Shole, D. G., & Belayneh, M. Z. (2019). The effect of side slope and clay core shape on the stability of embankment dam: Southern Ethiopia. In International Journal of Environmental Science and Technology (Vol. 16, Issue 10, pp. 5871–5880). Springer Science and Business Media LLC. https://doi.org/10.1007/s13762-019-02228-3

Siahdashti, M. J., Jean Côté, and Philippe Sirois. 2015. "Effect of grain size distribution on the hydraulic properties of unsaturated granite sand." In *15th Pan-American Conference on Soil Mechanics and Geotechnical Engineering*. https://doi.org/10.3233/978-1-61499-603-3-2180

Smith, A. (2024). *Innovative Reuse of Baltimore Harbor Dredged Material for Vegetative Earthen Berm Construction*, Master's thesis, University of Maryland, 111 p.

Sobti, J., & Singh, S. K. (2017). Hydraulic conductivity and compressibility characteristics of bentonite enriched soils as a barrier material for landfills. In Innovative Infrastructure Solutions (Vol. 2, Issue 1). Springer Science and Business Media LLC. https://doi.org/10.1007/s41062-017-0060-0

Tokunaga, T. K. 2009. "Hydraulic properties of adsorbed water films in unsaturated porous media." *Water Resources Research* 45: W06415. https://doi.org/10.1029/2009WR007734.

Topaloglu, S., Cetin, A., Dayioglu, A. Y., & Aydilek, A. H. (2024). Laboratory Testing of Ferrochrome Slag as an Aggregate in Porous Pavements. In Geotechnical Testing Journal (Vol. 47, Issue 1). ASTM International. https://doi.org/10.1520/gtj20220249

van Genuchten, M. Th. (1980). A Closed-form Equation for Predicting the Hydraulic Conductivity of Unsaturated Soils. In Soil Science Society of America Journal (Vol. 44, Issue 5, pp. 892–898). Wiley. https://doi.org/10.2136/sssaj1980.03615995004400050002x

Veeresh, H., S. Tripathy, D. Chaudhuri, B. C. Ghosh, B. R. Hart, and M. A. Powell. 2003. "Change in physical and chemical properties of three soil types in India as a result of amendment with fly ash and sewage sludge." *Environmental Geology* 43: 513–520. https://doi.org/10.1007/s00254-002-0656-2.

Vereecken, H., Weynants, M., Javaux, M., Pachepsky, Y., Schaap, M. G., & van Genuchten, M. Th. (2010). Using Pedotransfer Functions to Estimate the van Genuchten–Mualem Soil Hydraulic Properties: A Review. In Vadose Zone Journal (Vol. 9, Issue 4, pp. 795–820). Wiley. https://doi.org/10.2136/vzj2010.0045

Wang, J., François, B., & Lambert, P. (2017). Equations for hydraulic conductivity estimation from particle size distribution: A dimensional analysis. In Water Resources Research (Vol. 53, Issue 9, pp. 8127–8134). American Geophysical Union (AGU). https://doi.org/10.1002/2017wr020888

Yetimoglu, T., & Salbas, O. (2003). A study on shear strength of sands reinforced with randomly distributed discrete fibers. In Geotextiles and Geomembranes (Vol. 21, Issue 2, pp. 103–110). Elsevier BV. https://doi.org/10.1016/s0266-1144(03)00003-7

Zare, M., Afyuni, M., and Abbaspour K. C. 2010. "Effects of biosolids application on temporal variations in soil physical and unsaturated hydraulic properties." *J Residuals Sci Technol*. 7 (4): 227–235.

Zhang, Y.,Ghaly, E. A., Li, B. (2012). Physical properties of wheat straw varieties cultivated under different climatic and soil conditions in three continents. In american Journal of Engineering and Applied Sciences (Vol. 5, Issue 2, pp. 98–106). Science Publications. https://doi.org/10.3844/ajeassp.2012.98.106

Zibilske, L., W. M. Claphamm, and R. V. Rourke. 2000. "Multiple applications of paper mill sludge in an agricultural system: soil effects." *J. Environ. Qual.* 29: 1975–1981. https://doi.org/10.2134/jeq2000.00472425002900060034x.